Resilience Quantification of Transportation Infrastructure Subjected to Hazards

Resilience Quantification of Transportation Infrastructure Subjected to Hazard

By

Behfar Godazgar, M.Sc.

A Thesis Submitted to the School of Graduate Studies in Partial Fulfillment of the Requirements for the Degree Master of Applied Science

McMaster University

MASTER OF APPLIED SCIENCE (2022) (Civil Engineering)

McMaster University Hamilton, Ontario

TITLE:	Resilience Quantification of Transportation Infrastructure Subjected to Hazard
AUTHOR:	Behfar Godazgar, M.Sc.
SUPERVISOR:	Dr. Susan Tighe
CO-SUPERVISOR:	Dr. Georgios Balomenos
NUMBER OF PAGES:	i-63

Lay Abstract

Resilience quantification of infrastructures is the assessment and measurement of their ability to withstand and recover from disruptive events. However, there is a significant research gap in this field, with limited studies and standardized methodologies available.

This research presented a framework to quantify the hazard resiliency of infrastructures through development of resilience surface. The framework and the procedure were then numerically tested on a real bridge in Canada as a case study.

Abstract

Evaluating the resilience of transportation infrastructures, including bridges, roads, and tunnels, is a critical aspect of ensuring the ongoing functionality and reliability of urban or regional areas in the face of various disruptive events. Such infrastructures are susceptible to a range of disruptions which can have significant impacts on their ability to function effectively. Resilience refers to the capacity of an infrastructure or a system to withstand and recover from these disruptions. This research presents a framework to evaluate the resilience surface for assessing the resilience of various transportation infrastructure components. This comprehensive approach involves several steps. First, the framework identifies unique damage configurations by performing a fragility analysis. This analysis allows for a better understanding of how susceptible the infrastructure is to different hazards. Next, the framework focuses on the restoration of the affected infrastructure by developing recovery curves for each identified damage configuration. This is done by taking into account relevant restoration data and considering the specific characteristics of each configuration. Additionally, the framework acknowledges the inherent uncertainty that exists within various aspects of infrastructure resilience assessment. These uncertainties include hazard intensity, modeling uncertainty, and the restoration process itself. By incorporating these uncertainties into the framework, a more accurate and reliable assessment can be achieved. The utility of this framework is demonstrated through its application to a real-world case study involving a highway bridge located in Canada. The goal of this research is to offer decision-makers a valuable tool for evaluating the resilience of transportation infrastructure. This can contribute to more robust and reliable transportation infrastructures, capable of withstanding and recovering from a wide range of disruptive events.

Acknowledgement

First and foremost, I would like to express my heartfelt gratitude to my supervisor, Dr. Georgios Balomenos, and my co-supervisor, Dr. Susan Tighe. Their constant inspiration and direction have significantly enriched my academic and research journey. They were always there to offer help for my investigations and to provide support and motivation during challenging times. I would like to acknowledge the support and funding from a start-up funding provided by the Faculty of Engineering at McMaster University that made this research possible.

I would also like to express my sincere appreciation to my family and friends for their support and backing throughout my academic journey. A special mention goes to my wife, Mitra, whose unwavering support was with me in every challenging and exhilarating phase of this journey.

Table of Contents

List of Figures

List of Tables

Chapter 1: Introduction

1.1 Motivation

This research is conducted to enhance transportation infrastructure resiliency, which will ensure continuity of operations and minimize disruption in extreme events. In our societies, transportation infrastructure facilitates the movement of people, goods, and services. It can have severe societal and economic impacts if this system is disrupted by natural disasters or other unexpected events. By developing a robust framework to assess and improve the resilience of these infrastructures, we can better prepare for, respond to, and recover from these disruptive events. Ultimately, this research contributes to building safer, more reliable transportation infrastructures that can withstand a broad array of challenges.

1.2 Research objectives

In most cases, a restoration model is needed before assessing the resiliency of infrastructure subjected to hazards. It is typically assumed that simplified models will estimate the infrastructure's functionality during the restoration process, examples are the recovery curves presented in HAZUS (FEMA, 1999) for various damage states. One downside of this assumption is that there's no way to separate idle time from repair time since the models are designed for regional loss analysis instead of individual infrastructures. Moreover, simplified models typically fail to differentiate between various types of individual infrastructure (i.e., different bridge types) (Karamlou & Bocchini, 2017a). This is because most of these models are tuned based on the system damage state (i.e., the damage state of the bridge as a system), making the damage definition too qualitative, and not considering all damage configurations (DCs).

Therefore, to address the above challenges, the main goal of this research is to improve an existing framework to compute recovery curves for transportation infrastructure. Recently, Karamlou and

Bocchini (Karamlou & Bocchini, 2017a) presented a framework to develop probabilistic restoration curves for bridges, which was achieved by scheduling the required restoration tasks and creating the restoration schedule of the bridge. This framework is adopted in the present study and adjusted to account for uncertainties in the idle time in the recovery curves. In past studies, it has been shown that the uncertainty in idle time can significantly affect the recovery time of infrastructure (Capacci & Biondini, 2020; Decò et al., 2013) and should therefore be considered in resilience assessments. In the adjusted framework presented in this study, recovery curves are derived from restoration schedules rather than system damage states. For each DC, associated restoration characteristics, such as restoration tasks, precedence relations, required resources, and idle time are gathered. By scheduling the required tasks in the restoration schedule, the recovery curve for each DC is obtained. Next, the concept of resilience surface is explained, and an approach is presented for developing the resilience surface from recovery curves for each DC. Resilience surface is a graph that estimates the value of infrastructure's functionality after an extreme event with an intensity measure IM. Finally, this study aims to show the applicability of the proposed framework to an existing bridge in Canada.

The objective of this study can be summarized as follows:

- Improve upon the framework originally presented by Karamlou and Bocchini (2017a) for the development of probabilistic restoration curves for bridges. This will involve adjusting the framework to account for uncertainties related to idle time within recovery curves. This is an aspect shown to significantly influence recovery time in previous studies.
- Utilize the revised framework to create recovery curves based on restoration schedules rather than system damage states, incorporating restoration characteristics such as tasks, precedence relations, required resources, and idle time for each DC. With these recovery

curves, the concept of a resilience surface is further explained and an approach for developing such a surface is presented. The resilience surface is a graphical representation estimating the value of infrastructure functionality following an extreme event with an intensity measure (IM).

- Showcase the applicability and usefulness of this updated framework through a practical application to an existing bridge in Canada. This will validate the framework in a real-world scenario and allow for the assessment of its robustness, adaptability, and effectiveness in enhancing the resilience of transportation infrastructure.

1.3 Thesis organization

Chapter 1 of this thesis discusses underlying motivation and objectives for this research.

Chapter 2 presents a short summary of the conducted research and identifies the current gaps in the resilience quantification of transportation infrastructures.

Chapter 3 presents the concept of resilience surface and a formulation to develop the surface for transportation infrastructures. It also introduces the proposed framework for developing the resilience surface based on the restoration curves of each DC.

Chapter 4 presents the applicability of the proposed framework in the resilience quantification of transportation infrastructures by developing the recovery curves and resilience surface for a highway bridge in Canada.

Chapter 5 discusses the conclusion of the conducted research based on the obtained results and presents some suggestions for future research.

Chapter 2: Literature review

2.1 Resilience

The idea of resilience is widely used in several scientific and engineering fields whenever the impact of an external stressor, such as man-made or natural hazards, on a system is the topic of discussion. In civil engineering fields, resilience is defined as the capability of a structure or infrastructure to minimize the chance of any disturbance, mitigate the associated impacts in case of a disturbance and recover from it to an acceptable level of performance in a timely and effective manner (Bruneau et al., 2003; Hollnagel et al., 2006). Bruneau et al. (Bruneau et al., 2003) identified 4 key characteristics of a resilient system, including robustness, rapidity, resourcefulness, and redundancy.

Robustness is defined as the capacity of a system to withstand a certain level of demand or stress without major functionality degradation. In most cases, robustness is determined by the amount of damage incurred or the loss of functionality caused by the hazard. For example, in bridge engineering, incurred damage can be recognized as damage to the bridge elements, such as column cracking or failure, abutment spalling and bearing dislocation, which will result in a specific extent of functionality loss such as limiting the permitted traffic capacity or closing the bridge entirely until restoration is performed. Rapidity refers to the degree to which a system recovers from any disturbance in functionality. It depends on the extent of damage, resource availability, and local practice. Rapid recovery reduces system downtime, which is essential for measuring indirect costs while damaged components are restored. Resourcefulness is described as the capacity to recognize problems, set priorities, prepare resources, and apply restoration methods, when a disrupting condition exists that compromises the system's functionality. A resourceful system can take advantage of available resources (i.e., physical, informational, and monetary) and human resources

to carry out restoration and meet functionality goals. Lastly, redundancy is the replacement ability of system components when the functionality is altered or noticeably degraded. Redundancy can be considered as a way to enhance system resilience by providing redundant materials and components (Argyroudis, 2022). For example, Echevarria et al. (2016) suggests that redundant material and members enhances bridge resilience. In the case of a road network, Ganin et al. (2017) proposed alternative routes as a feasible solution to boost the resilience.

2.2 Resilience curve

In this context, resilience curves are commonly used to illustrate the progression of functionality over time for a given disturbance. An example is presented conceptually in Figure 1. t_0 represents the occurrence of an extreme event which triggers the infrastructure to lose its normal functionality. Functionality loss depends on the robustness of the structure, and it is less when robustness is higher. The extreme event may cause several components of the infrastructure to be damaged, rendering the infrastructure inaccessible for a period of time. For example, a highway bridge's traffic capacity may be lowered to 50% by closing multiple lanes. t_r denotes the start of the restoration process where the restoration and repair procedure of the damaged infrastructure is initiated. At this step, the repair crews and technicians are effectively using a variety of available resources and executing different restoration tasks to neutralize the impact of damaged components (Karamlou & Bocchini, 2017a). The time between $\mathrm{t_0}$ and $\mathrm{t_r}$ is called idle time when no physical restoration work is performed. Instead, investigatory and preparation tasks, such as visually inspecting the asset for damage, designing restoration works, and preparing resources, are usually performed during idle time. The duration and variability of idle time typically depend on resource availability, the extent of damage, and local preparedness and could affect the restoration time of the infrastructure significantly (Mitoulis et al., 2021).

Finally, time t_1 denotes the end of the restoration process. This is where the functionality recovers to its initial level, i.e., to the infrastructure state just before the hazard occurrence. The duration of the restoration process relies on several uncertain elements, including, but not limited to, the damage level (e.g., the number and degree of damaged components), availability of resources (e.g., the availability of the resources when they are required) and local practice (e.g., a guide to how repairs should be conducted) (Mitoulis et al., 2021).

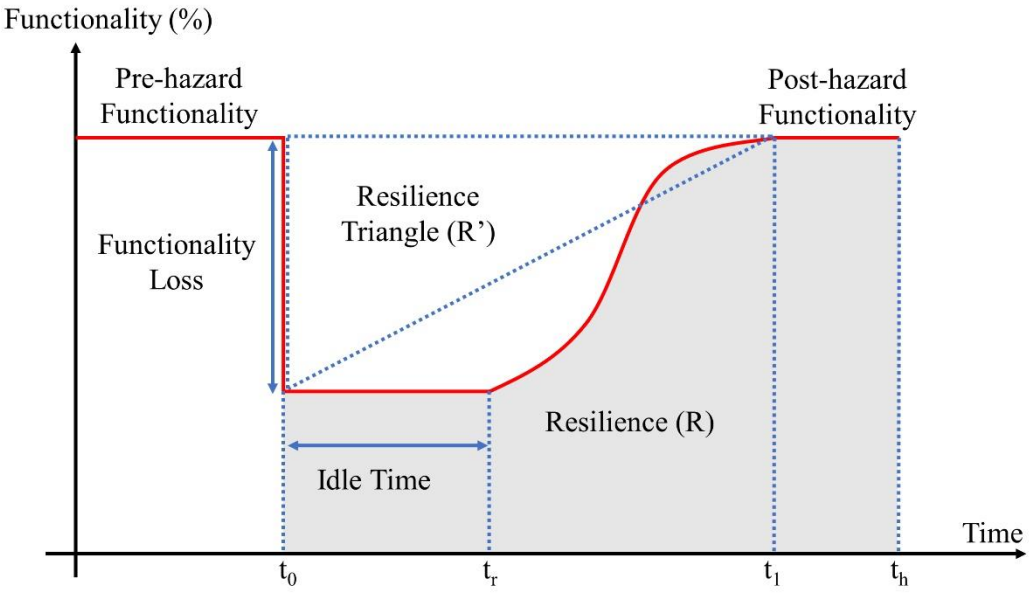

Figure 1 Schematic representation of a resilience curve

There are several indicators that can be used to quantify an infrastructure's resilience. In this regard, Bruneau et al. (2003) quantified resilience for the first time and identified the resilience triangle as a metric to quantify the loss of resilience (R′), as shown in Figure 1. This means that the larger the area enclosed by the triangle, the lower the system's resilience (R). This definition is presented mathematically in Eq. (1).

$$R' = \int_{t_0}^{t_1} [100 - Q(t)]dt \quad (1)$$

The quantification of resilience can be normalized based on a specific time interval, thus letting decision makers prioritize asset restoration. As an example, Cimellaro et al. (2009) normalized the resilience index based on the restoration time shown in Eq. (2), while Minaie and Moon (2017) suggested using one year as a control time for calculating the resilience index. However, when resilience is quantified based on the area under or outside the resilience curve, it is possible that different systems with different restoration scenarios have the same resilience index. As an example, a bridge with a small loss of functionality and low importance may be repaired longer than a bridge with a considerable loss of functionality and high importance. To address this issue, Zobel (2011) presented the adjusted resilience function reflecting the different perspectives of decision makers. This model considers the upper limits of the tolerable level of restoration time and functionality loss as per the owner's perception.

$$R = \frac{\int_{t_0}^{t_1} Q(t)dt}{t_1 - t_0} \tag{2}$$

Other researchers presented resilience metrics with a higher complexity level. Argyroudis et al. (2020) identified repair cost as a metric for resilience assessment of bridges, considering direct cost, indirect cost due to detour, and socioeconomic effects of traffic disruption due to bridge closure. By recognizing gradual functionality drops even before extreme events occur, Ayyub (2014) proposed resilience metrics considering aging infrastructure. Lastly, Sharma et al. (2018) introduced a set of mathematical equations describing the statistical properties of resilience curves, such as resilience quantile, resilience moment and skewness.

2.3 Restoration models

Restoration models give the functionality of components or systems after the occurrence of an extreme event. An accurate analysis of the functionality is necessary for a realistic resilience

assessment since the resilience is typically presented as the evolution of functionality over time. This case is often neglected in the resilience analysis of infrastructures since simplified restoration models are suggested for functionality after an extreme event, while sophisticated models are used to capture the system response during the event. It is commonly considered that the development of restoration functions is challenging due to difficulties such as human factors, uncertainty related to the repair process, and available resources. Despite this difficulty, there are several notable restoration models in the literature addressing the functionality evolution of transportation infrastructures during the repair process. This section summarizes and categorizes the restoration functions.

2.3.1 Categories

Available restoration models in the literature are often categorized based on their characteristics and the method utilized to develop them. Survey-based models are derived depending on the results of numerous surveys and inquiries collected from bridge professionals (Padgett & DesRoches, 2007) while mathematical models are often generated by assuming a mathematical function that is consistent with the expected restoration profile of the structure and calibrating that function based on the available data (Bocchini et al., 2012). In another category of restoration models, the functionality/closure of the bridge throughout the repair process is presented based on the damage condition of a single component (Porter, 2004) while others present functionality evolution by considering numerous damaged components or configurations (Karamlou & Bocchini, 2017a). Finally, probabilistic models define functionality as a random parameter by considering multiple uncertainty factors in the modeling and repair process, such as initial damage status, resource availability, and repair task duration (Karamlou & Bocchini, 2017a). On the other

hand, deterministic models present functionality over time with deterministic output (Padgett & DesRoches, 2007).

2.3.2 Overview of restoration models

In 1985, ATC-13 (1985) provided restoration data for various types of structures and infrastructure, including transportation services. Based on a survey, the restoration data presented the mean and standard deviation of the elapsed time required to reach 30%, 60%, and 100% of normal functionality levels for each class. Damages were classified according to their severity, including no, slight, light, moderate, heavy, major, and destroyed. In the case of bridges, ATC-13 categorized highway bridges into two groups based on span length, such as major bridges with spans over 100 feet and conventional bridges.

HAZUS (FEMA, 1999) classified four damage states for the development of restoration models, namely minor, moderate, slight, and extensive. The restoration function for each damage state, presented in Figure 2, was derived by fitting the normal cumulative distribution function (CDF) to ATC-13 data. For the computation of the functions, slight, light, moderate, and heavy damage states were used for the conventional bridges explored in ATC-13.

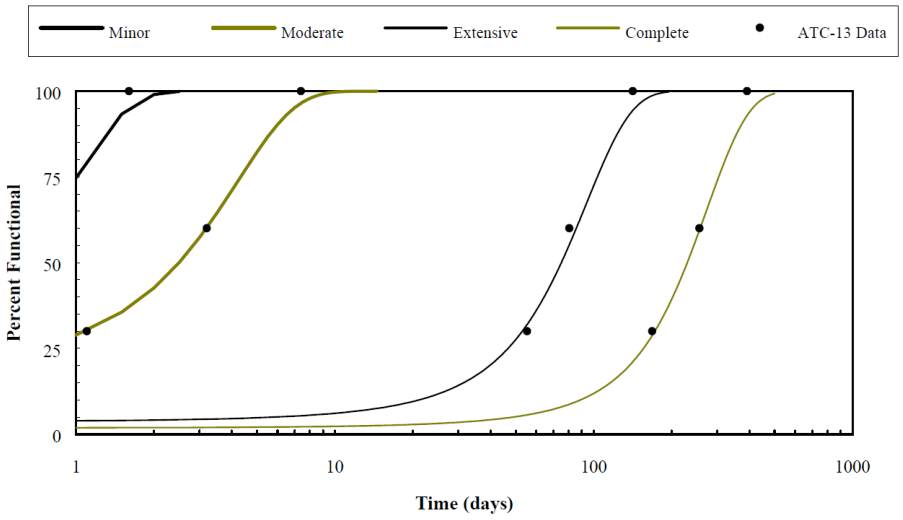

Figure 2 Bridge restoration functions in HAZUS (FEMA, 1999)

Porter (Porter, 2004) carried out a survey to estimate the likelihood of concrete bridges being closed or partially closed. This was based on damage to certain components, such as settlement in approaches and spalling in backwalls. Decision variables included whether to reduce traffic lanes or close the bridge for full restoration, or in case of bridge closure, whether the closure duration is brief (about 3 days) or extended. Lognormal CDFs were employed to represent the results in the form of fragility functions, giving the probability of bridge closure conditioned on component damage. Figure 3 presents an example of the fragility function giving the probability of bridge closure when approach settlement occurs.

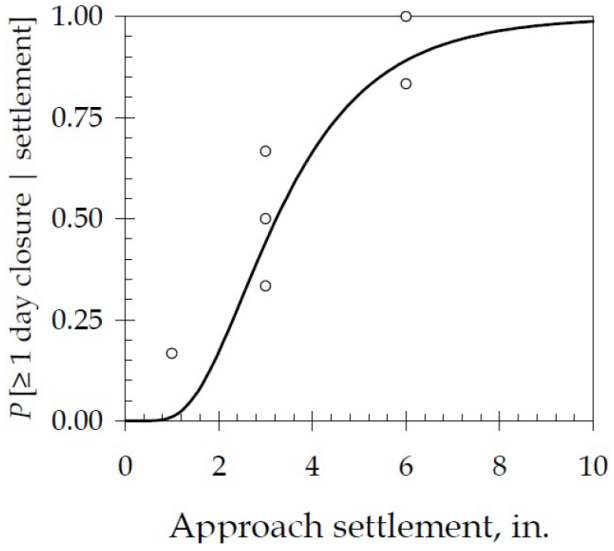

Figure 3 Restoration function for bridge settlement in (Porter, 2004)

Padgett and DesRoches (2007) surveyed 28 bridge experts and officials on the condition of bridges in the central and southeastern US. The results were shown in the form of stepwise functions that represent the bridge traffic carrying capacity following the restoration process. These functions are depicted in Figure 4. The description of damage states was adopted from HAZUS (FEMA, 1999). It should be noted that similar to HAZUS (FEMA, 1999), different

bridge types had the same restoration functions as long as the description of damage states was the same.

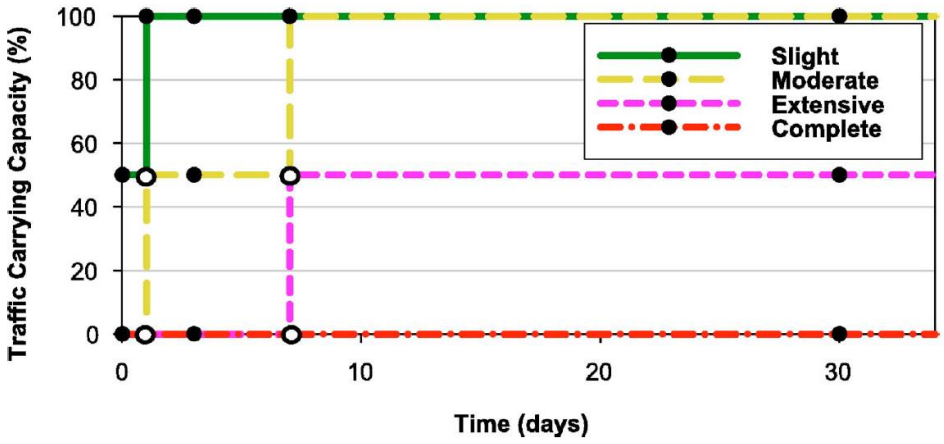

Figure 4 Stepwise restoration function developed by (Padgett & DesRoches, 2007)

In 2012, Bocchini et al. (2012) proposed a sinusoidal-based restoration model, presented in Figure 5, that can model different recovery and restoration shapes, such as linear, trigonometric, and exponential, suitable for assessing different systems' resilience. Six random variables represent various characteristics of the proposed model, such as residual functionality, idle time, and target functionality. Despite the model's versatility and ability to model a variety of restoration scenarios, calibrating its parameters can be challenging, since a variety of uncertain circumstances and subjective decisions influence their outcome, such as available resources, prioritization of repair tasks and the community's preparedness.

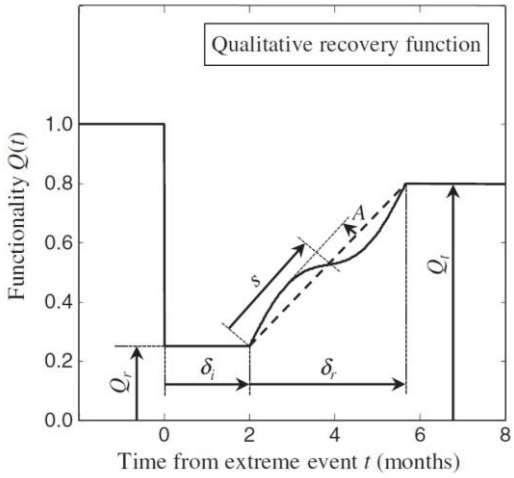

Figure 5 Sinusoidal resilience curve presented in (Bocchini et al., 2012)

Karamlou and Bocchini (2017a) modeled the probabilistic restoration curves of highway bridges in the US by simulating the bridge recovery schedule in detail and considering uncertainty in incurred damage configurations, task duration, resource availability, and resource consumption. Two levels of bridge functionality were considered for developing the restoration curve, including partial and complete bridge closure. Results are presented as a probabilistic curve showing that functionality (or loss of functionality) exceeds levels of functionality thresholds. Karamlou and Bocchini (2017b) also presented the functionality-fragility surface of the studied bridge pictured in Figure 6, which is defined as the conditional probability of functionality (or loss of functionality) for the time after the occurrence of the extreme event and the event intensity.

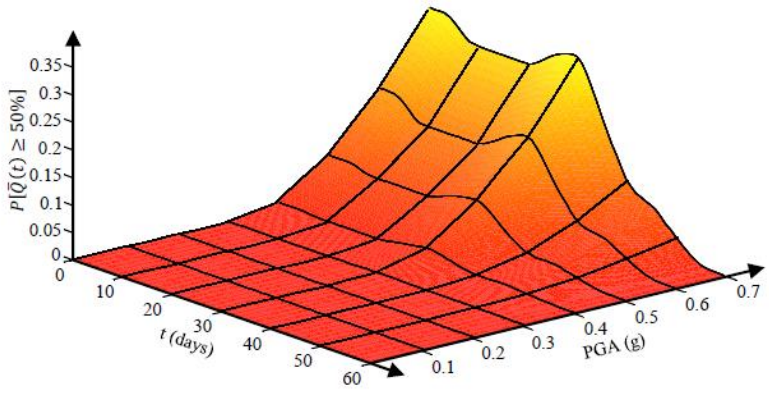

Figure 6 Functionality-fragility surface presented in (Karamlou & Bocchini, 2017b)

2.4 Overview of resilience frameworks

A variety of methodologies and frameworks have been developed to gauge the resilience of various structures and infrastructures, highlighting the diversity of approaches and metrics used in these assessments. Chan and Schofer (2016) developed a graphical and analytical metric to gauge the resilience of a railway transit system affected by weather disruptions. Study results provided valuable insights into the mitigation strategies and adaptive capacities that are necessary in these settings based on the application of resilience analysis to railway transit systems and the specific impacts of weather events. Huang et al. (2022) suggested a framework for evaluating the resilience of tunnels, especially those constructed in alluvial deposits and exposed to earthquakes. In a similar vein, Bešinović (2020) undertook a thorough examination of resilience in railway transport systems, taking into account both infrastructure and operations. An additional key contribution to this field was made by Omer et al. (2012), who proposed a comprehensive three-stage framework to boost maritime transportation infrastructure resilience. This methodology, specifically developed for maritime settings, can serve as a model for enhancing resilience in other industries. A different approach was taken by Balomenos et al. (2019), who investigated the impact of a hurricane on transportation networks. As part of their research, they analyzed communities' ability

to access health care services after disruption, highlighting the interdependence of transport networks and healthcare access, as well as the importance of resilient infrastructure. Bocchini et al. (2014) developed a unified approach to quantifying the resilience of civil structures and infrastructures to resilience. As a result of their work, more precise recommendations and interventions can be made due to the quantitative element that they add to the assessment. Argyroudis et al. (2020) adopted a cost-based perspective for their resilience assessment framework. They developed a method to quantify the resilience of bridges exposed to earthquakes based on direct and indirect losses. This financially focused approach emphasizes the economic implications of infrastructure resilience, presenting a comprehensive view of disaster recovery costs. Similarly, Mackie et al. (2016) assessed bridge resilience from an environmental perspective, using carbon footprint as a performance metric. As a result, infrastructure has become increasingly aware of its environmental impacts and its resilience, bringing sustainability into the conversation about resilience. Finally, Chandrasekaran and Banerjee (2016) combined resilience considerations with economic analysis. Based on resilience and retrofit cost as the criterion, they determined optimal retrofit configurations for highway transportation infrastructure, showing how resilience, cost-effectiveness, and infrastructure improvements can be integrated.

Beyond various models and indices, the incorporation of resilience principles into infrastructure planning, evaluation, and enhancement procedures is gaining momentum. Organizations such as the Federal Highway Administration (FHWA) and Departments of Transportation (DoTs) are beginning to embed these concepts into their operational strategies. For instance, the FHWA has developed a guide entitled 'Vulnerability Assessment and Adaptation Framework' (Filosa et al., 2017), detailing a strategic method for detecting potential threats, applying countermeasures, and setting up surveillance systems. Similarly, California's Department of Transportation (Caltrans)

conducted an examination of climate change's impact on resilience (Crow et al., 2014), highlighting the importance of building resilient infrastructure to counter climate-related risks. By adopting this proactive approach, Caltrans aims to safeguard the state's transportation infrastructure from potential threats and to ensure its enduring viability.

Chapter 3: Proposed framework

3.1 Resilience surface

3.1.1 Concept

Figure 7 shows an illustration of the resilience surface. Resilience surface shows the gradual increase in infrastructure functionality over time following extreme hazards. Additionally, it shows a decrease in functionality as the Intensity Measure (IM) increases. The resilient surface shown in Figure 7 is only an expected shape, which will vary widely depending on the type of infrastructure studied, the development method, and the available data. It is also important to take into account the nature of the hazard and its consequences on the infrastructure before choosing the IM. In the seismic damage analysis of bridges (Padgett et al., 2008) and railway bridges (Yilmaz et al., 2021), Peak Ground Acceleration (PGA) has been found to be the best IM. Or in the case of flood-induced scour, commonly the scour depth is the recommended IM for bridge damage analysis (Mitoulis et al., 2021). Multi-hazard scenarios, such as floods and earthquakes (Argyroudis & Mitoulis, 2021), where two or more IMs contribute to the damage, can utilize a hypersurface in multi-dimensional space rather than a three-dimensional surface. For example, Balomenos and Padgett (2018) explored the effects of wave loads on the fragility analysis of wharves exposed to hurricanes by developing a 4D fragility surface (i.e., three optimal IMs).

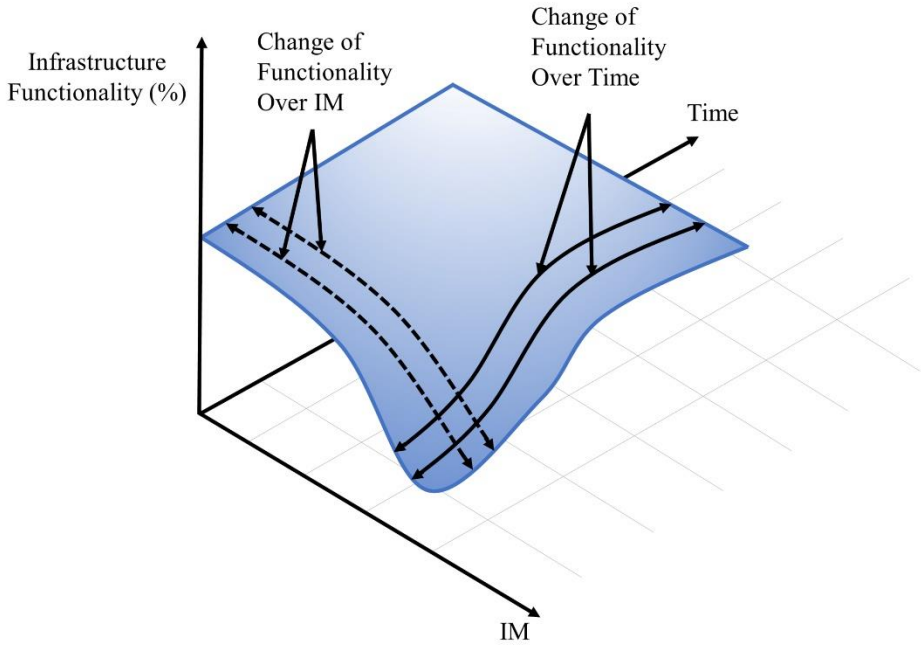

Figure 7 An illustration of the resilience surface

3.2 Formulation

In resilience quantification of transportation infrastructures, the functionality evolution Q_t of an infrastructure over time (t) is evaluated as (Bocchini et al., 2014)

$$Q(t) = \sum_{i=0}^{N_{DS}} Q[t|DS_i]P[DS_i|IM] \quad (3)$$

where $Q[t|DS_i]$ is the infrastructure recovery curve for each unique Damage State (DS_i) versus time, and $P[DS_i|IM]$ is the occurrence probability of each DS_i in each IM. $P[DS_i|IM]$ is typically determined by analyzing the fragility of the system, considering various factors such as uncertainty in hazard , response, and capacity of the infrastructure. Recovery curves $Q[t|DS_i]$ can, however, be challenging to develop due to several uncertainties involved in the restoration analysis such as unknown restoration duration, idle time, and available resources. In this regard, commonly simplified models, such as the recovery curves discussed in HAZUS (FEMA, 1999), are employed to predict the infrastructure's functionality after a disaster. The problem is most of the available

recovery models are created based on system damage state. This might not capture all possible DCs. Additionally, there is no way to distinguish idle time from true restoration time since the current recovery models have been designed for regional assessment rather than for individual infrastructure types (i.e., for an individual bridge) (Karamlou & Bocchini, 2017a).

This paper proposes a methodology for addressing the above-mentioned challenges by establishing resilience surfaces for infrastructures as

$$Q(t) = \sum_{i=0}^{N_{DC}} Q[t|DC_i]P[DC_i|IM] \quad (4)$$

where for a given infrastructure, $Q[t|DC_i]$ is the recovery curve of unique damage configurations (DC_i), and $P[DC_i|IM]$ is the probability of each DC over each IM. A DC is a combination made up of a number of damaged parts whose reduced functionality affects the functionality of the entire infrastructure. Bridges, for example, may have DCs that include several damaged columns/abutments/bearings. The advantage of using DC to develop the recovery function, over the use of the system damage state, is that in this way many uncertain factors can be taken into account in the restoration analysis that were previously not possible. Thus, uncertain factors associated with the restoration process can be considered for each DC. Restoration duration, resource availability, and idle time are some of these factors. Following this, different restoration tasks can be scheduled, and the restoration schedule can be developed for the infrastructure to estimate its functionality during repair process.

3.3 Proposed framework

There are two major components to the framework for developing the resilience surface, i.e., the fragility analysis component and the restoration analysis component, which are further elaborated in the subsequent sections (Figure 8).

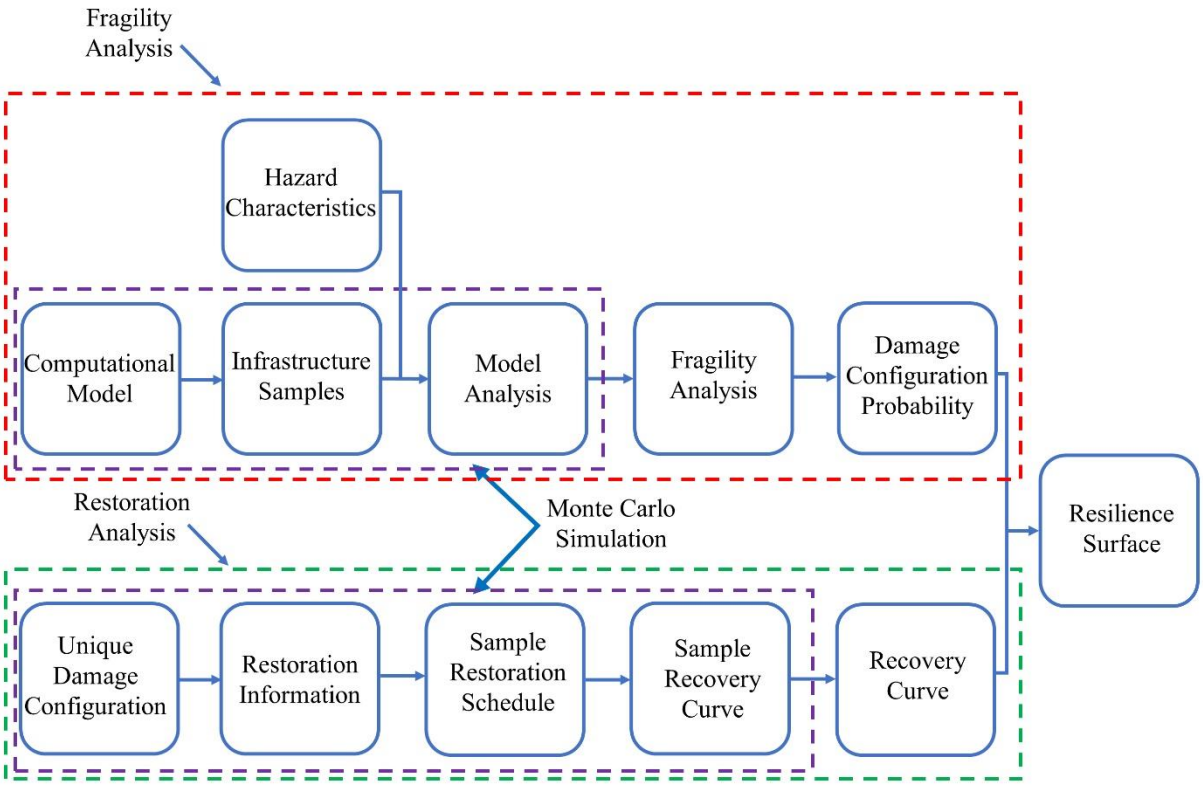

Figure 8 An overview of the development process for a resilient surface

3.3.1 Fragility analysis

In the fragility analysis component, randomness related to hazard intensity (e.g., PGA for earthquakes, scour depth for floods, etc.) is taken into account. In addition, the infrastructure response is estimated considering the inherent uncertainties in materials and modeling properties (e.g., uncertainty in steel and concrete strength). It begins with the step "Computational Model," where a detailed model of the infrastructure is developed to simulate its performance during a hazard. In the step “Infrastructure Samples”, Latin Hypercube Sampling (McKay et al., 2000) is used to generate samples of the material and modeling properties using predefined infrastructure properties. Since random properties vary significantly between different types of infrastructure, they are usually determined by the available information on the system. In this process, random samples are generated and then assigned to a computational model in order to generate

infrastructure samples that are statistically significant, yet nominally identical. Beyond the infrastructure under investigation, data concerning the hazard, including its nature and severity, are also essential for fragility analysis. For this reason, the step labelled "Hazard Characteristics" involves collecting pertinent information for each hazard. This information is then utilized in conjunction with the infrastructure model in the subsequent stage. In the step "Model Analysis," the created computational model is then subjected to the hazard based on an analysis technique (e.g., Nonlinear Time-History Analysis for earthquakes) and the response of its key components are recorded. In the step “Fragility Analysis”, infrastructure components' responses (e.g., displacements, forces, etc.) are compared to repair-based damage states to determine if the examined damage states have been violated. To restore the functionality of infrastructure components, repair-based damage states are thresholds above which specific restoration tasks are required. In this way, damage states are linked to demand parameters that determine how components are restored. Damage states from each "Model Analysis" specify a specific combination of damaged components, which here are referred to as DCs. It is common for DCs to occur more than once, so the first occurrence of each DC is filtered from the pool of DCs. As a final step, "Damage Configuration Probability" calculates the probability that a given DC will arise among all the analysis samples, and it is stored in a separate array for the recovery curve computation.

3.3.2 Restoration analysis

A unique sample of infrastructure DC (previously evaluated in the fragility analysis component) is used in the restoration analysis component's step "Sample Damage Configuration" (Figure 8). During the step "Restoration Information", for each sample DC, the available literature and expert opinions are used to gather the associated restoration information. “Restoration Information” is

typically subdivided into two parts: “Restoration Task” and “Idle Time”. The restoration task consists of the construction and design tasks required to repair the damaged component. To define a restoration task, three sets of information are usually needed. The first set of information is the "Duration Distribution" of the "Restoration Task", assuming that several factors, such as crew proficiency, weather conditions, and equipment efficiency, influence the duration of each task. Thus, it is crucial to consider uncertainty in the duration of each task by generating Latin Hypercube samples based on the probability distribution of each restoration task. "Precedence Relations" is the second set of information that defines the order of the different restoration tasks, as well as the common construction methods used to put them in order. In the case of a damaged bridge, it is often necessary to repair the foundation before repairing the columns. The third set of information is "Required Resources", which describes which construction resources are required for carrying out a restoration task (e.g., manpower, machinery, etc.). The “Idle Time” is the other part of the “Restoration Information” (Figure 9). In previous studies (Capacci & Biondini, 2020; Decò et al., 2013), idle time uncertainty has been shown to influence infrastructure recovery duration significantly. Additionally, idle time is believed to increase as infrastructure suffers greater damage, since the owners must assess the damage before starting the restoration process (Argyroudis S et al., 2019). Thus, by using Latin Hypercube Sampling, duration samples are generated based on a probabilistic distribution of idle time (McKay et al., 2000). In the next step, the bridge restoration schedule will be developed using these duration samples and other restoration information.

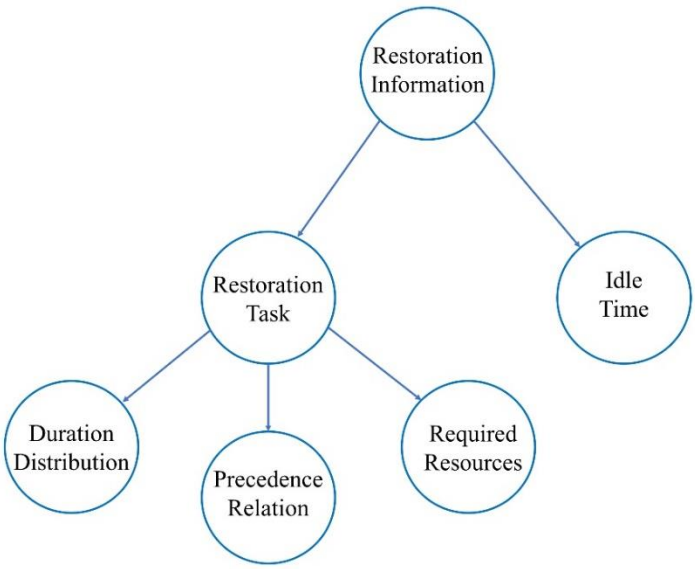

Figure 9 Information required for restoration of a damaged infrastructure

Based on the framework proposed in (Karamlou & Bocchini, 2017a), samples of infrastructure restoration schedules are computed in the step "Sample Restoration Schedule" (Figure 8). It is not within the scope of this study to explain in detail how restoration schedules are developed, so only a brief description is provided. A schematic representation of the sample restoration curve is shown in Figure 10a. Through a project scheduling technique, generated samples of idle time, task duration, available resources, and precedence relations are utilized to construct a sample restoration schedule (Artigues et al., 2013). The restoration schedule samples represent restoration scenarios that are feasible and likely to occur based on uncertainties regarding restoration task durations, resources, and idle time. Rather than finding the best possible restoration schedule, this step aims to identify all possible restoration scenarios based on the uncertainty factors. Next, the time window for executing each restoration task in the "Sample Restoration Schedule" is determined by satisfying the precedence relations between each restoration task and resource consumption (i.e., at any given time interval, the resources required cannot exceed the resources

available). In the next step, based on the "Construction-induced Functionality (Q_{task})" and "Structural Safety (Q_{safety})" requirements, the infrastructure functionality is estimated in each time window (Figure 10b and c).

As a result of damage to one (or multiple) components, the "Structural Safety" requirements estimate the infrastructure's functionality. An example would be if all columns in a bent were to fail, the road traffic is reduced to zero and the bridge is no longer able to carry traffic. In "Construction-induced Functionality" requirements, the infrastructure's functionality is estimated based on the safety of the restoration crew. Due to the safety of the repair crew, some tasks may require closing or partially closing the infrastructure. The repair crew may reduce traffic capacity by up to 50% when working on a highway bridge deck, allowing the workers to work safely and effectively.

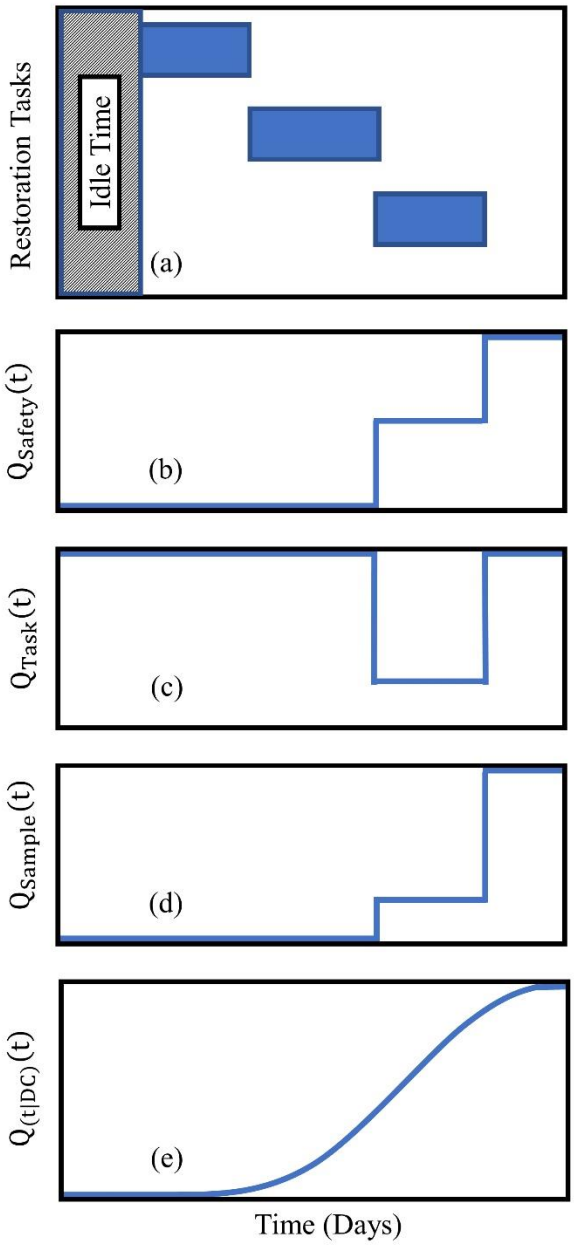

Figure 10 Schematic representation of the development process of the recovery curves

Referring to Figure 8, in step "Sample Recovery Curve", functionality versus time is plotted for the investigated sample to obtain the stepwise recovery curve Q_{sample} (Figure 10d). For one sample of the restoration schedule, the stepwise recovery curve depicts the expected infrastructure functionality after the hazard occurrence. Thus, for all generated samples of idle time and the

duration of restoration tasks, the restoration schedule computation is repeated for each generated sample., and Q_{sample} is calculated for each generated sample. As a last step, the mean functionality is calculated among all sample recovery curves to determine the DC's recovery curve (i.e., $Q[t|DC_i]$) in (4) (Figure 10e).

DCs may differ depending on the type of infrastructure in the fragility analysis. It is therefore necessary to repeat the restoration analysis component for all other unique DCs in order to obtain their recovery curves. The recovery curves show the resilience of the infrastructure across a wide range of scenarios, and are comparable to HAZUS curves, but with detailed consideration of uncertainties specific to the type of infrastructure examined. Finally, Eq. (4) calculates the resilience surface of the infrastructure that has been exposed to a specific hazard.

To demonstrate the versatility of this framework, it's essential to highlight that although the case study emphasizes bridge infrastructure and seismic hazards, the methodology is adaptable and can accommodate various types of infrastructure and hazard scenarios. Despite differences in structural components, hazard demand parameters, and restoration procedures among different infrastructures and hazards, the core principles of the proposed framework remain consistent. For each type of infrastructure, it's necessary to define repair-based damage states and demand parameters that align with their structural features and expected performance under the considered hazard conditions. In the same vein, for various hazard types, the framework flexibly adjusts to synchronize demand parameters, capacities, and restoration tasks to the specifics of the hazard. The wide-ranging applicability of the proposed methodology establishes it as a comprehensive tool for resilience assessment across a diverse array of infrastructures and hazards. In addition, while the present study centers primarily on the resilience of a singular infrastructure, its findings offer insights into the broader understanding of resilience at a network level. The framework set

forth serves as a foundation that can be expanded to incorporate the interdependencies within a network, which could influence restoration times if multiple components fail concurrently. This idea parallels previous research, such as that conducted by Balomenos et al. (2019), which analyzed the impact of bridge failure on network accessibility. The intricacy of these interdependencies underscores the significance and potential applicability of the current study in larger network scenarios.

It is also important to underscore that although the current study is centered on operational factors impacting restoration, the authors recognize the profound importance of economic implications. Nevertheless, the evaluation of restoration costs is not included within the purview of this particular investigation.

Chapter 4: Case Study

In the aftermath of natural or manmade disasters, bridges play a crucial role in ensuring transportation infrastructure functions effectively (Rinaldi et al., 2001). For example, when an extreme hazard strikes, a functioning bridge network will become a crucial component of emergency response teams' capacity to reach the affected areas in a timely manner (Balomenos et al., 2019; Bernier et al., 2019). Furthermore, by allowing the distribution of construction materials, repair crews, and equipment rapidly, an accessible bridge also has the potential to speed up the restoration process for other damaged structures and infrastructures (Karamlou & Bocchini, 2017a). In the past, however, several earthquakes, including those in 1994 Northridge (Hall et al., 1994), 1995 Kobe (Comartin, 1995), and 2011, Christchurch (Wilkinson et al., 2011), have shown that bridges may not be able to maintain their expected functional characteristics. For this reason, the assessment and quantification of the resilience of bridges that are exposed to earthquakes is crucial for community safety, the continuity of services, and the quality of life.

4.1 Bridge Description and Numerical Model

In order to demonstrate the suitability of the proposed framework, the procedure for the development of the resilient surface is implemented for the Chemin des Dalles Bridge in Trois-Rivières, Quebec, Canada, which has been the subject of a series of studies (Abdelmaksoud et al., 2022; Noade & Becker, 2019; Roy et al., 2010; Siqueira et al., 2014; Tavares et al., 2013). Based on the recovery curves presented in HAZUS (FEMA, 1999), a preliminary analysis of the seismic resilience of this bridge has recently been performed by Godazgar et al. (2021). The present study, on the other hand, extends the seismic resilience assessment by calculating the recovery curves and the resilience surface by relying on the DCs that are found in each unique bridge construction.

Figure 11 illustrates the schematic representation of the examined bridge, which measures 106.5m long by 13.2m wide by 6.2m high. Six Type VI AASHTO girders support the concrete deck of the superstructure. Using elastomeric bearings, the girders transfer the load from the superstructure to the piers and abutments. The continuous deck of the bridge is supported by two concrete piers and two seat-type abutments. Three circular reinforced concrete columns with bent beams form the piers' rigid frames in the transverse direction. Foundations for piers and abutments rest on soil types C according to the National Building Code of Canada (NBCC) (National Research Council of Canada (NRCC), 2015). There is a pinned connection between the columns of the right piers and the spread footings, while the left columns are rigidly connected.

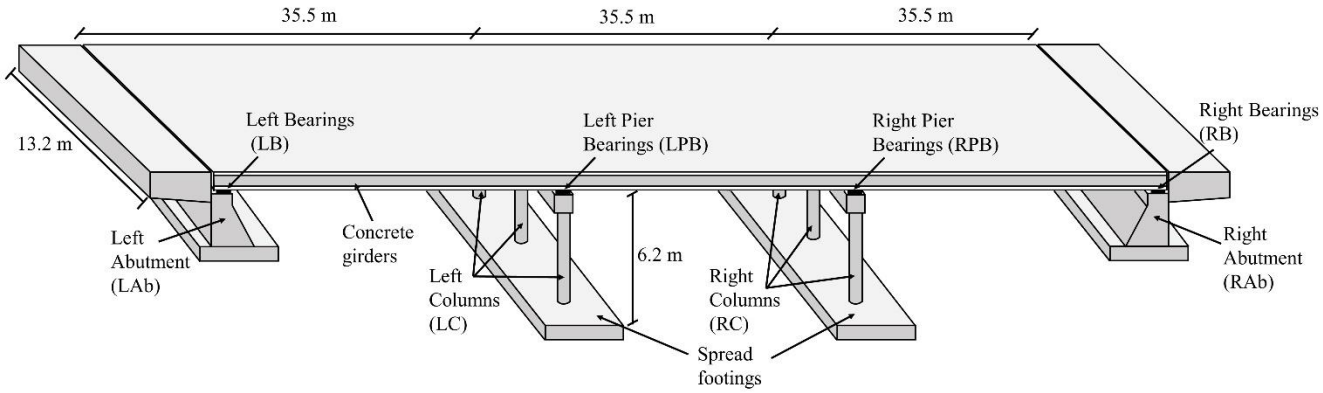

Figure 11 An illustration of the Chemin des Dalles bridge located in Trois-Rivières, Quebec

In order to carry out a fragility analysis of the infrastructure, it is required to create a computational model of the infrastructure, as discussed in the previous chapter. To accomplish this, a detailed finite element model of the bridge was developed using OpenSees (Mazzoni et al., 2006) software, which is a comprehensive finite element model of the bridge, primarily based on the components that make up the bridge's response, including the deck, elastomeric bearings, columns, abutments, and spread footings. This model has been developed in 3D as a means of fully capturing the response of the structure to the ground motion. Considering that the superstructure remains elastic,

the deck and girders of the bridge were modeled using a grillage (Hambly, 1991). In order to verify the accuracy of this assumption, the displacements and forces of the deck and girders were monitored. The cross-sectional area of the deck and the girders, as well as the elastic modulus and shear modulus, were taken from Tavares et al. (2013). Models of elastomeric bearings were created using zero-length elements with bilinear material models based on their stiffness, yield, and ultimate strength adopted from (Tavares et al., 2013). Elastic beam-column elements were employed in order to simulate bent beam behavior. To simulate the columns, force beam-column elements with fiber sections were used. To determine the behavior of the column materials, the Concrete02 and Steel02 models in OpenSees were used, as well as the equation presented by Cusson and Paultre (1995) to define the confined and unconfined properties of concrete in the column. Based on the model developed by Wilson (1988) as well as Crouse et al. (1985), translational and rotational springs have been used to model the abutments. To simulate the behavior of the spread footings, each footing has been modeled in 3D with 3, 5, and 9 nodes in the longitudinal, transverse, and vertical directions, respectively. In Biazar et al. (2022), as well as Tavares et al. (2013), more details regarding the bridge modeling can be found.

As part of the fragility analysis, many material and modeling features were considered random variables in order to account for uncertainties. It was found that the variability of the selected parameters affected the bridge's estimated response. This was achieved by Latin Hypercube Sampling (McKay et al., 2000), which was used to create 30 samples of material properties, and to then link these samples to the bridge model to produce statistically significant, yet nominally identical bridge samples. A summary of all the random variables along with their distribution attributes has been given in Table 1 based on the work of Tavares et al. (2013). Moreover, previous studies have shown that the angle of earthquake incidence can significantly change the response

and behavior of highway bridges as a result of an earthquake (Banerjee Basu & Shinozuka, 2011; Torbol & Shinozuka, 2014). In order to determine the angle of earthquake incidence and the associated probabilistic distribution of the magnitude of the earthquake, several factors need to be taken into consideration, such as the location of the structure and the characteristics of the seismic faults found in the area. However, due to the absence of such data for the studied region, the angle of the earthquake incidence has been taken into account as a random variable uniformly distributed between 0 and π as illustrated in Table 1.

Table 1 Random variables included in fragility analysis

Random variables	Distribution characteristics			Units
Concrete Strength	Normal	$\mu = 28$	$\sigma = 4.3$	MPa
Steel Strength	Lognormal	$\lambda = 6.13$	$\zeta = 0.08$	MPa
Bearing Initial Stiffness	Uniform	$L = 0.5$	$U = 1.5$	Factor
Abutment passive initial stiffness	Uniform	$L = 0.5$	$U = 1.5$	Factor
Abutment active initial stiffness	Uniform	$L = 0.5$	$U = 1.5$	Factor
Mass variability	Uniform	$L = 0.5$	$U = 1.5$	Factor
Damping	Normal	$\mu = 1.3$	$\sigma = 0.06$	%
Earthquake angle of incidence	Uniform	$L = 0$	$U = \pi$	Radian

4.2 Ground Motion Selection

It is also important to note that the variability of the Ground Motion Time Histories (GMTHs) is another important source of uncertainty that is crucial in the analysis of seismic fragility of infrastructure. There are several factors to consider in choosing GMTHs: the earthquake source, wave propagation, soil conditions, etc. Since strong ground motion records for the Quebec region

in Canada are not available, artificial ground motions were used for the seismic fragility analysis. In this regard, Atkinson (2009) devised artificial ground motions to match NBCC (National Research Council of Canada (NRCC), 2015) uniform hazard spectra for different soil types in eastern Canada. In the artificial GMTHs developed by Atkinson (2009), four bins are considered in terms of magnitude and distance from the site, including Magnitude 6 at a distance of 10-15 km (bin 1) and 20-30 km (bin 2), and Magnitude 7 at a distance of 15-25 km (bin 3) and 50-100 km (bin 4). Thus, the fragility analysis was conducted using 24 bidirectional GMTHs (6 GMTHs from each bin).

4.3 Seismic Fragility Analysis

Seismic fragility analyses were conducted using the method proposed by Karamlou and Bocchini (2015). To this end, ten levels of IM for the selected GMTHs were specified, with PGAs ranging from 0.1g to 1.0g. Next, all 30 bridge samples were subjected to each scaled ground motion. A total of 720 time history analyses were conducted at each PGA level to estimate and record the bridge components' responses. To specify the states of damage of the bridge components, the response of columns, abutments, and elastomeric bearings was recorded. Using Tavares et al recommendations (Tavares et al., 2013), the displacement ductility of the left and right columns was calculated as the demand parameter. Using Mackie et al 's recommendations (Mackie et al., 2008), the demand parameters for elastomeric bearings and abutments are the maximum absolute displacement of the bearing and the maximum longitudinal displacement of the abutment, respectively. Boxplots are provided in Figure 12 for all the components studied for the result of seismic fragility analyses. In the boxes, the top and bottom edge show 75% and 25% of the demands, while the whiskers at their ends show the maximum and minimum of these values. Each box contains a horizontal line which represents the median demand at each PGA. When the bridge

is subjected to ground motions with higher PGA, it is apparent that the median demand on the bridge components is increased as a result of the stronger ground motions. The right columns in Figure 12a are found to exhibit higher demands in comparison with the left columns in Figure 6a. This is due to the fact that the right columns are linked to their associated foundations with a pinned connection. Furthermore, it can be observed that the uncertainties involved in fragility analysis, such as the modeling parameters, the variability in GMTH as well as the angle of incidence associated with them, have a significant impact on the dispersion of the component demands, especially at high PGAs. In Figure 6b, for example, it is clear that the dispersion of the abutment response at PGAs of 0.9g or 1.0g is considerably higher than that at PGAs of 0.5g or 0.6g. This displacement of the bearings can be seen in Figure 6c, with the elastomeric bearings on the piers having higher demands. Using the result of seismic fragility analyses, the repair-based damage states of the components are determined in the next step.

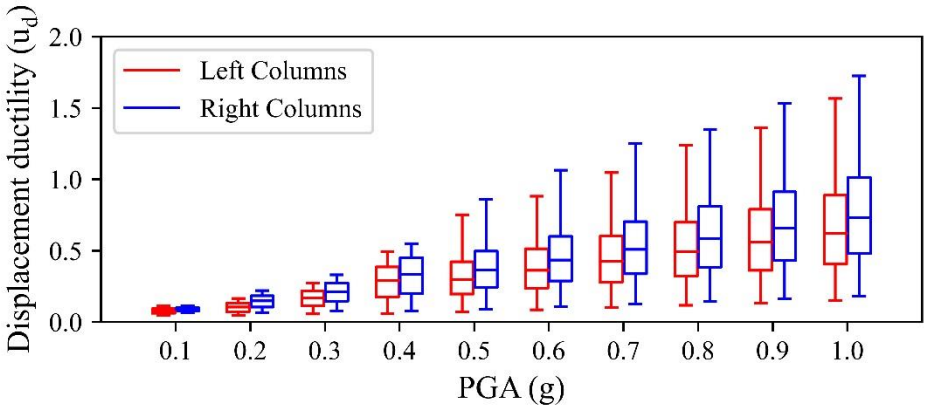

(a)

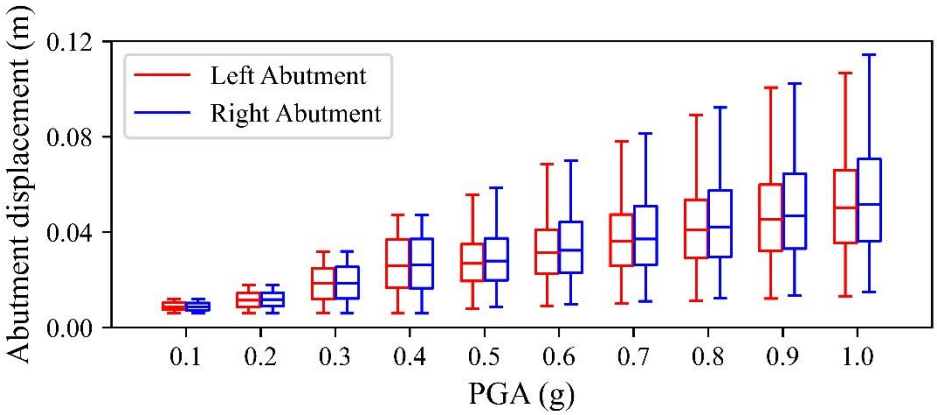

(b)

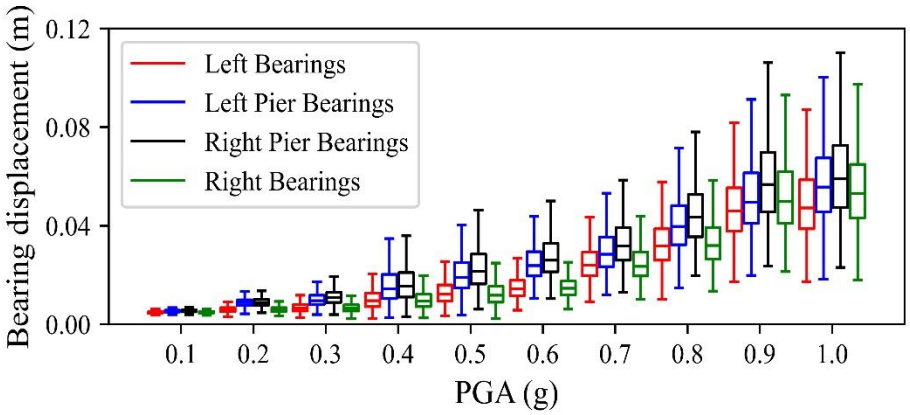

(c)

Figure 12 Result of seismic fragility analysis for column a), abutment b), and elastic bearing c)

Table 2 presents the repair-based damage states, taken from (Mackie et al., 2008; Tavares et al., 2013), along with their distribution parameters such as median S_C and logarithmic standard deviation β_C. In addition to describing the damage state, the restoration solution and restoration tasks used to restore the component to its original state are also provided in Table 2. Unlike the conventional damage states in HAZUS (FEMA, 1999), the repair-based damage states in this study are directly related to the associated restoration tasks. Therefore, elastomeric bearings do not have a repair-based damage state between yielding and failure. The reason for this is that it is typically

more cost-effective to replace a damaged elastomeric bearing rather than repair it. (Mackie et al., 2008).

Table 2 Restoration tasks associated with repair-based damage states

Component	DS	Criteria		Damage Description	Restoration Solution	Restoration Tasks
		S_C	β_C			
Columns, displacement ductility (μ_d)	DS1	1.08	0.25	Cover concrete spalling	Minor patching	{2, 3}
	DS2	1.76	0.46	Longitudinal bar buckling	Major patching	{2, 3}
	DS3	3.00	0.46	Column failure	Replace column	{1, 4, 6, 12, …, 18}
Elastomeric Bearings, maximum displacement (m)	DS1	0.07	0.25	Bearing yielding	-	-
	DS2	0.15	0.25	Bearing Failure	Replace bearing	{1, 4, 5, 6}
Abutments, maximum displacement (m)	DS1	0.10	0.25	Damage to joint seal	Replace joint seal	{11}
	DS2	0.12	0.30	Backwall cracking	Repair backwall	{7, …, 11}
	DS3	0.14	0.30	Extensive backwall damage	Replace backwall and approach slab	{7, …, 11, 19, …, 22}

Using time history analysis in each PGA, the damage states of each component were determined by comparing the results with the repair-based damage states in Table 2. For each repair-based damage state, capacity samples were generated based on a Latin Hypercube sampling technique (McKay et al., 2000) using the lognormal distribution to describe the damage states. For better understanding of the fragility analysis results, for each of the studied bridge components, Figure 7 illustrates the probability that each damage state (i.e., DS1, DS2) will occur at different PGAs. For example, the diagram shows that no bridge component will be damaged when the bridge is subjected to ground motions less than 0.4 (g). Intensities greater than 0.4 (g) will result in some damage to the columns, and intensities greater than 0.8 (g) will cause some damage to the elastomeric bearings and abutments, but no component of the bridge will experience DS 3.

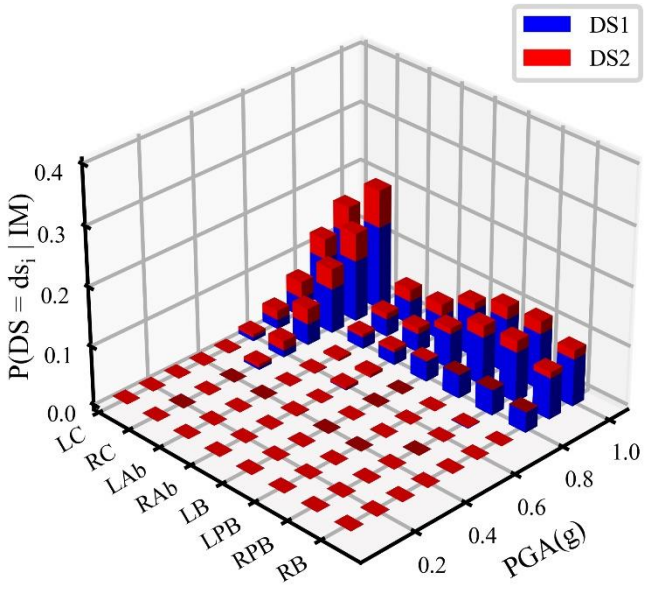

Figure 13 Damage state probability for each bridge component

4.4 Restoration Analysis

In each time history analysis, a DC represents the damage state of the bridge components. It is common for DCs to occur more than once in different time history analyses. From the pool of DCs, the first occurrence of each DC has been extracted, and the probability of that DC occurring at each of the PGAs ($P[DC_i|IM]$) has been calculated. Afterwards, for each DC, Table 3 was used to extract the restoration tasks and the relevant properties. The properties include duration distribution, required resources and construction-induced functionality (Q_{task}). A duration distribution based on engineering judgments was assumed for each damage state in the restoration analysis to account for idle time, summarized in Table 4. In order to schedule the restoration tasks correctly, samples of task duration and idle time were generated, and prioritization relations (Karamlou & Bocchini, 2017b) were used to determine the order in which the tasks should be executed. As well as this, the total amount of resources required for each restoration task in Table 3 should not exceed the available resources at that point in time.

Table 3 Restoration tasks with their properties (adopted from (Karamlou & Bocchini, 2017a, 2017b; Mackie et al., 2008)

Task #	Task description	Duration				Required resources				Q_{task} (%)
		Min	Max	Mode	Type	Crew	Geo-machine	Crane	Concrete machine	
1	Submit/review temporary support	20	40	30	Trigonometric	0	0	0	0	100
2	Repair column spalls	3	9	6	Trigonometric	2	0	0	1	100
3	Repair column cracks with epoxy	3	9	6	Trigonometric	2	0	0	1	100
4	Install temporary support	1	3	2	Trigonometric	5	0	1	0	0
5	Install replacement bearing	1	2	-	Uniform	5	0	0	0	100
6	Remove temporary support	1	1	-	Uniform	5	0	1	0	0
7	Excavate abutment	1	2	-	Uniform	5	2	0	0	50
8	Repair abutment cracks with epoxy	1	3	2	Uniform	2	0	0	1	100
9	Repair abutment spalls	1	3	2	Trigonometric	2	0	0	1	100
10	Abutments backfill	1	4	2	Trigonometric	5	2	0	0	50
11	Install abutment joint seal assembly	1	3	2	Trigonometric	3	0	0	1	50
12	Submit/review bridge removal plan	10	20	15	Trigonometric	0	0	0	0	100
13	Remove existing column	3	6	-	Uniform	5	0	1	0	100

14	Place column reinforcement	3	6	-	Uniform	5	0	1	0	100
15	Place column forms	3	3	-	Uniform	5	0	1	0	100
16	Pour column concrete	3	6	-	Uniform	5	0	1	2	100
17	Cure concrete	7	12	10	Trigonometric	2	0	0	0	100
18	Remove column forms	1	1	-	Uniform	2	0	1	0	100
19	Remove ½ backwall and approach slab	1	3	2	Trigonometric	5	1	1	0	50
20	Construct ½ backwall	1	3	2	Trigonometric	5	0	1	2	50
21	Construct ½ approach slab	1	2	2	Trigonometric	5	1	0	1	50
22	Construct ½ backwall and approach slab	1	3	2	Trigonometric	5	0	1	2	50

Table 4 Idle time distributions based on trigonometric functions

DS	Min (days)	Max (days)	Mode (days)
1	5	30	15
2	10	40	30
3	20	60	40

As discussed before, availability of resources can influence how long it takes to restore the bridge. As an example, performing restoration tasks might take a longer time if one of the resources is unavailable (e.g., a crew member or machinery). Therefore, it is essential to account for uncertainty in the available resources in restoration analysis. For this purpose, Table 5 presents distribution parameters for the available resources, which are treated as random variables that follow a uniform distribution.

Table 5 Distribution of available resources (Karamlou & Bocchini, 2017b)

Available resources	Min	Max
Crew	5	10
Geo-machine	2	4
Crane	1	2
Concrete machine	1	2

To illustrate the framework for developing recovery curves, a sample restoration schedule is developed for a DC whose left and right columns are in DS1, its right pier bearings are in DS1, and its right abutment is in DS2. The restoration schedule for the studied DC is shown in Figure 14a. The sample schedule was created by random numbers generated from the associated distributions to calculate restoration task duration (Table 3), idle time (Table 4), and available

resources (Table 5). After idle time (hatched areas in the restoration schedule), the left and right columns will be repaired for spalls (task 2) and cracks (task 3). Due to the bearing restoration process, submit/review temporary support (task 1) also commences at the beginning. Afterwards, elastomeric bearings in the right pier are replaced (task 5) and the right abutment is repaired (tasks 7 through 11). This sample schedule lasts 54 days in total.

The next step involves estimating the bridge's functionality during restoration based on structural safety (Q_{safety}) and construction-induced functionality (Q_{task}). Due to the damage to the components, the Q_{safety} limits the functionality of the bridge, making it structurally unsafe. In this case, each component of the bridge is assumed to have a certain functionality level (e.g., 0% or 50%), summarized in Table 6. Hence, at each time interval, the bridge functionality is reduced by the functionality levels of different damaged components so long as they have not been restored or replaced. Figure 14b, for example, shows that when the right pier bearings are repaired, the bridge functionality based on the structural safety requirement (Q_{safety}) increases from 0% to 50% on day 40, and after the restoration tasks for the right abutment are completed, the bridge functionality increases to 100%. Next, in order to provide safe working space for the repair crew, Q_{task} requirements limit bridge functionality during each restoration task. This is accomplished by adopting the Q_{task} values from Table 3 for each restoration task and assigning them to the time intervals of the restoration schedule when that task is being executed. Figure 8c, for example, illustrates the variation in bridge functionality versus time for the studied DC based on construction-induced functionality requirements (Q_{task}). Next, for each of the time intervals studied in Figure 14d, the minimum value between Qsafety and Qtask is chosen as the sample recovery curve (Q_{sample}). According to Figure 14d, the bridge functionality will be 0% up until day 41 in this sample restoration schedule. After day 41, the bridge functionality increases to 50%, meaning the

bridge is half open, and the bridge is fully functional after day 54, when the restoration process comes to an end. As mentioned earlier, it is possible that the restoration process duration and the resulting recovery curve differ from sample to sample due to uncertainties regarding the duration of the tasks, the available resources, and idle time. The process of Figure 8(a-d) is repeated for 1000 samples with uncertain parameters, and the mean bridge functionality is calculated for all sample recovery curves. As an example, Figure 8e shows the mean recovery curve ($Q[t|DC]$) of the DC studied. A gradual increase in recovery can be seen on the recovery curve from day 38 until the end of the study for the studied DC, whose average restoration duration was 52 days.

Table 6 Structural safety requirements for bridge components' functionality (Karamlou, 2017)

Component	DS	Functionality level for Q_{Safety}
Columns	DS1	50
	DS2	50
	DS3	0
Elastomeric bearings	DS1	0
Abutments	DS2	50
	DS3	0

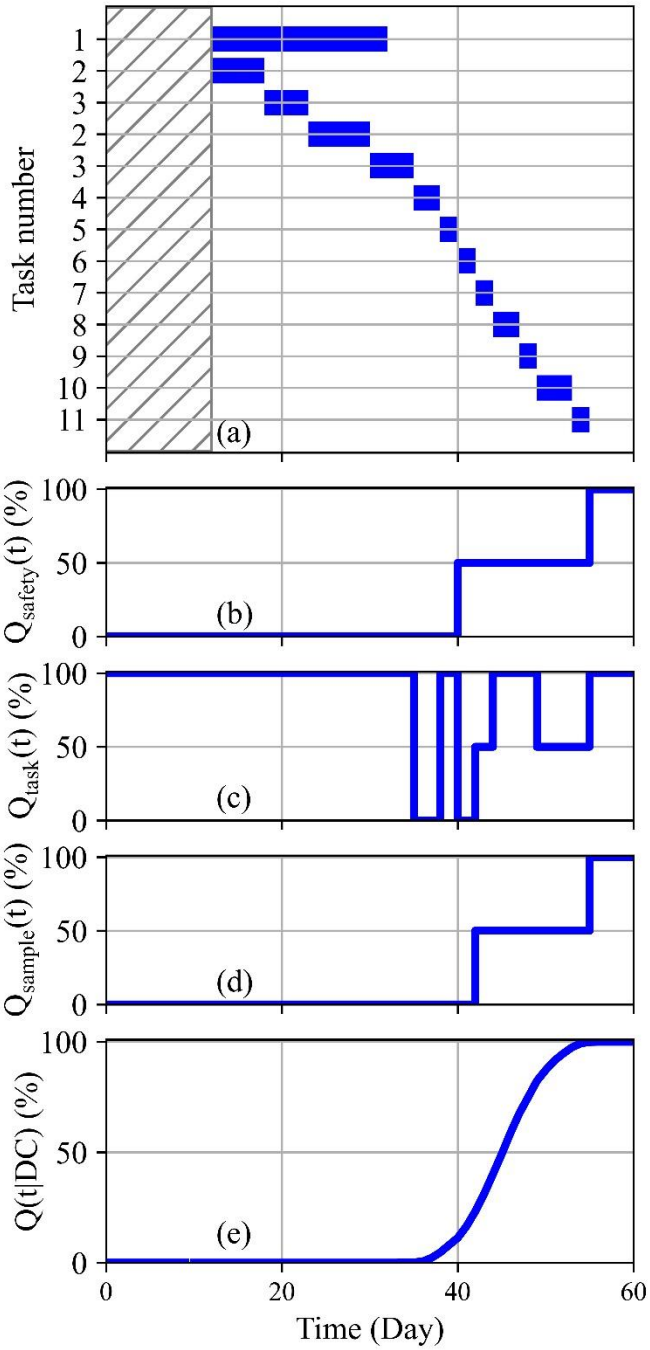

Figure 14 Studied DC along with restoration curves a) restoration schedule sample, b) bridge functionality based on the structural safety requirement, c) bridge functionality based on the construction-induced functionality, d) step-wise recovery curve for the sample schedule, e) recovery curve for the DC

Based on the fragility analysis of the bridge, 10 unique bridge DCs were identified and categorized into major and minor DCs. Minor DCs suffer damage to the extent that the bridge is half open

(50% functionality) after the earthquake. Meanwhile, major DCs suffered damage to such an extent that the bridge is completely closed after the earthquake (0% functionality). It is also noteworthy to mention that the occurrence of DS1 in the elastomeric bearings and the subsequent replacement of the bearings caused the bridge to completely close as no other components (columns or abutments) experienced DS3 (Figure 7). Therefore, pre-earthquake repair or replacement of the elastomeric bearings may be an effective solution here in order to prevent the bridge's total closure during restoration (Aria & Akbari, 2013).

In relation to the uncertainty associated with functionality, Figure 15 depicts the standard deviation for each day during the repair process. It is evident that the dispersion is more pronounced from day 38 through day 52. This can be ascribed to the execution of primary restoration tasks that significantly impact functionality during this period, hence leading to a higher variability in functionality compared to other phases of the repair process.

4.5 Development of Recovery Curves and Resilience Surface

Based on the proposed framework, Figure 16 shows the recovery curves ($Q[t|DC_i]$) for 10 unique bridge DCs, of which 7 are minor and 3 are major. It should be noted that 2 recovery curves for minor DCs overlap because the restoration duration is similar. There is a horizontal line at the beginning of the recovery curves, indicating that the functionality has remained constant during that time (i.e., 50% functionality for the minor DCs and 0% functionality for the major DCs). A portion of this time is due to idle time when only investigation and inspection tasks are being performed instead of restoration activities. Moreover, functionality does not increase immediately after restoration tasks are initiated and executed, which contributes to the constant functionality period at the beginning of recovery curves. In fact, for the functionality to increase, several tasks

must be completed and several components repaired. A similar pattern was observed in Figure 14d, where functionality increased when restoration tasks for columns and bearings are performed.

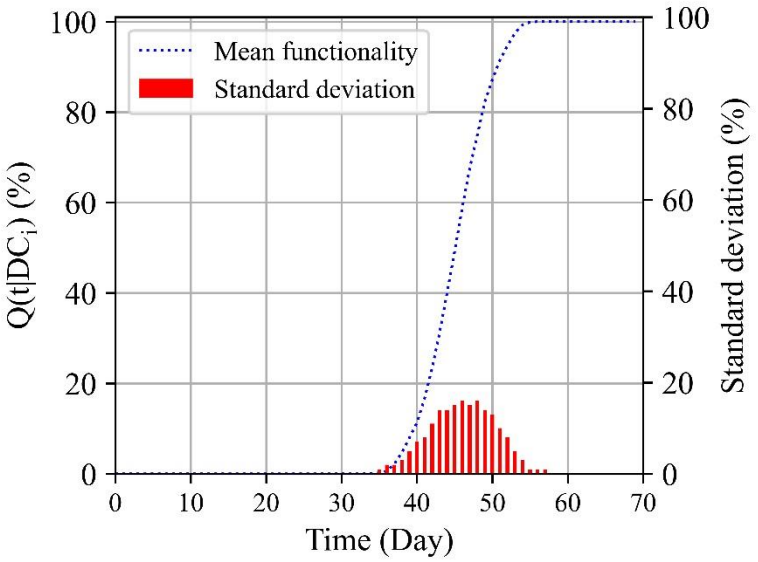

Figure 15 Standard deviation for the studied DC

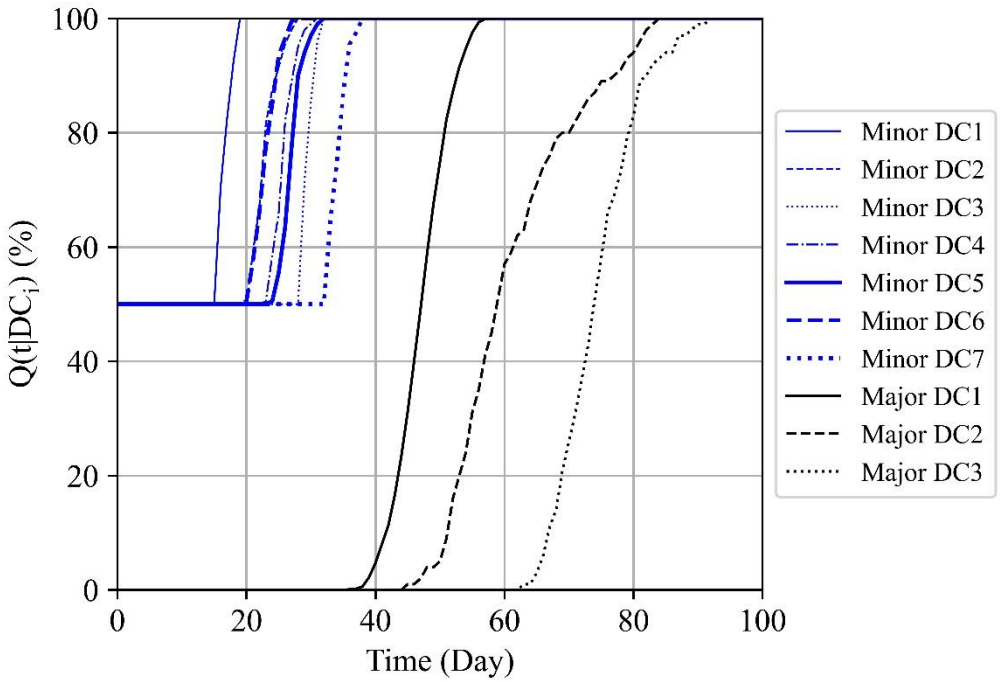

Figure 16 Bridge recovery curve for minor and major DCs. A complete list of all DCs is presented in the Appendix.

In order to develop the resilience surface of the studied bridge, the results of the fragility analysis ($P[DC_i|IM]$) and the restoration analysis ($Q[t|DC_i]$) were combined with Equation (4). The resilience surface, shown in Figure 17, illustrates how the studied bridge performs over a wide range of PGAs. Based on the computed resilient surface, the studied bridge subjected to ground motion with a PGA below 0.4 (g) is expected to remain fully open (100% functionality). Moreover, if the examined bridge is subjected to ground motions with a PGA greater than 0.9 (g), it will require 80 days to fully open (100% functionality).

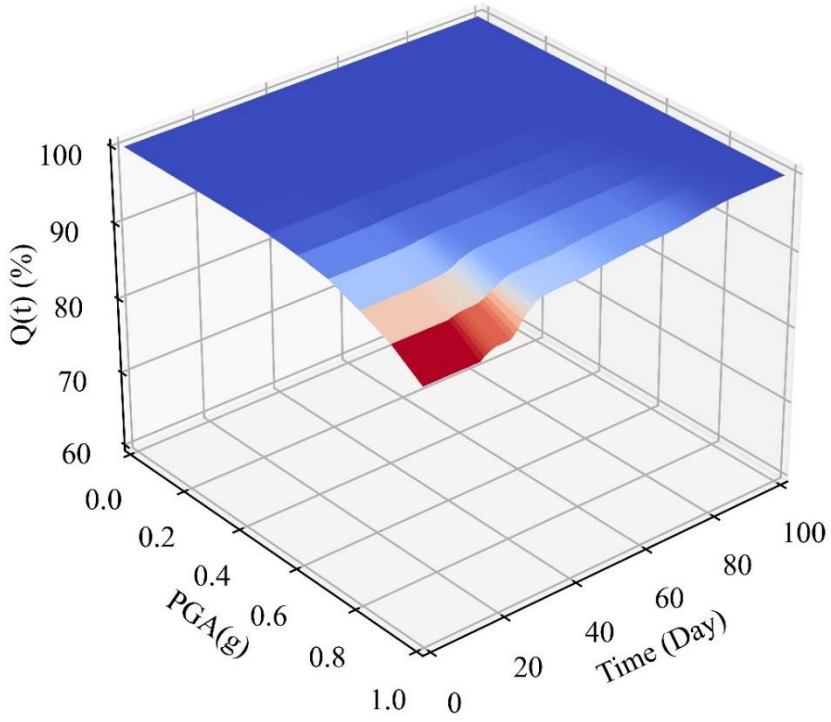

Figure 17 Resilience surface of the studied bridge

The resilience surface can be used to gain further insight by plotting the evolution of functionality over time and PGA. This is shown in Figure 18(a-b). In Figure 18a, the bridge is expected to maintain more than 90% functionality even during seismic events with high PGA values (e.g., 0.9

or 1.0 (g)). Furthermore, it has been concluded that functionality of the bridge in the early stages of restoration (around 20-30 days) is driven by minor DCs with rapid increases in functionality. Towards the end of restoration, however, bridge functionality is dictated by the major DCs with slow increases in functionality. It's noteworthy, as depicted in Figure 18a, that both low and high PGA intensities result in approximately the same expected restoration durations (around 80 days). In instances of low intensity, the overall repair duration is extended due to the influence of significant damage configurations and their associated likelihoods of occurrence. Conversely, in high intensity situations, even though the damage is substantial, the concurrent restoration of multiple components reduces the total recovery time. This observation underscores the critical role of effective restoration planning, and is in accordance with findings from previous studies, such as those conducted by (Karamlou & Bocchini, 2017b). Figure 18b shows that the bridge functionality does not increase significantly in the first 20 days following the earthquake (It is important to note that 0 days and 10 days overlap). These periods are controlled by idle time and the execution of early restoration tasks, neither of which causes the bridge to become more functional. Figure 18b illustrates that 30 days after the earthquake, a noticeable improvement in the bridge's functionality can be expected.

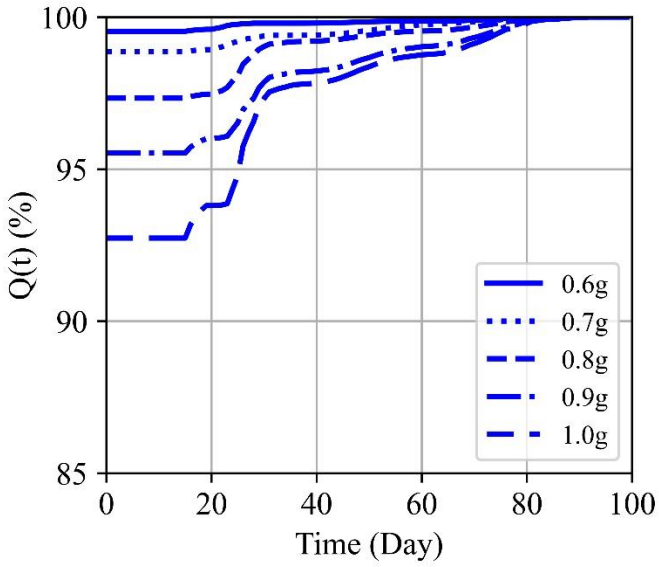

(a)

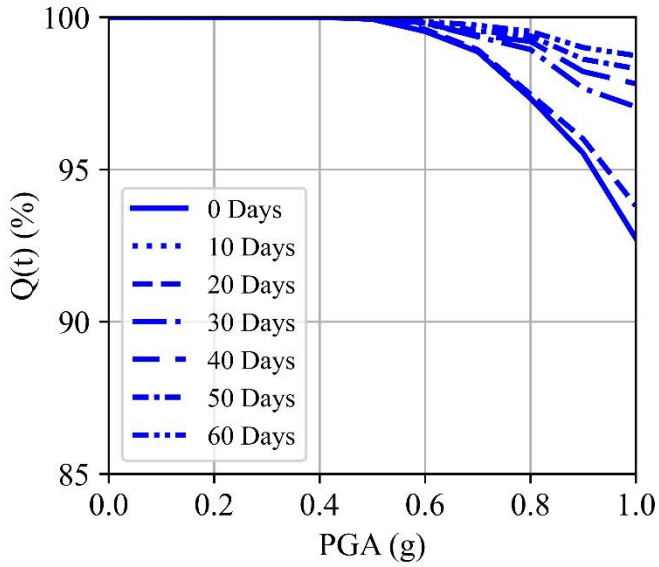

(b)

Figure 18 Bridge functionality evolution by a) time, b) PGA

As a means of encapsulating the restoration and functionality of the studied bridge, the resilience index for a period of 100 days is calculated using Equation (1). Figure 19 shows the resilience index of the studied bridge versus PGA. In seismic events whose PGAs are up to 0.5 (g), the resilience index is 100%, which indicates that there is no functionality loss, and no restoration is

required. With the increase of the PGA, the resilience index drops sharply, representing a loss of functionality for the studied bridge, which requires restoring it. In addition, NBCC (National Research Council of Canada (NRCC), 2015) specifies that the PGA for the bridge location corresponding to 2% exceedance probability is 0.285 (g). Thus, according to the presented resilience index, the examined bridge can be expected to perform well under the design earthquake chosen by the National Building Code (National Research Council of Canada (NRCC), 2015).

The resilience index presented in this research provides a quantitative gauge of the bridge's capability to withstand and recover from seismic events over a time span of 100 days. A resilience index of 100% signifies no loss in functionality, implying no need for restoration efforts. As the resilience index decreases, it signifies an equivalent decrease in functionality, indicating a need for restoration. The establishment of a resilience threshold for decision-making is dependent on the specific demands and tolerability to functional loss of the stakeholders. For example, a resilience index of 85% or more could be deemed acceptable, representing minimal functional loss and swift recovery. In the provided case study, the bridge exhibits resilient performance for the design PGA in accordance with NBCC, displaying a resilience index of 100%. For higher PGAs, the corresponding reduction in resilience index necessitates a careful assessment by decision-makers to consider whether further mitigation actions or enhancements are warranted.

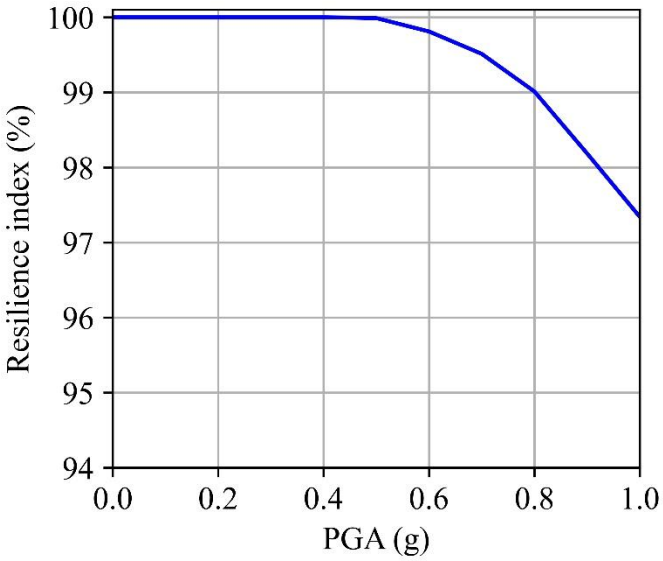

Figure 19 Bridge resilience index for different PGAs

Chapter 5: Conclusion and future work

5.1 Summary of thesis

This study puts forth an innovative framework, devised to assess and quantify the resilience of transportation infrastructure, crucial to the sustainability and functionality of urban environments. The method for resilience quantification involves the formulation of a resilience surface that is achieved through evaluating the recovery curves of distinct demand and capacity scenarios. The resilience surface represents a graphical depiction of how the infrastructure reacts to and recovers from disruptive events, providing a comprehensive view of the infrastructure's resilience under varying conditions.

The proposed approach merges the analysis of fragility and restoration, incorporating the inherent uncertainties that occur within the parameters of demand, capacity, and restoration properties. Fragility analysis, in this context, is the quantification of the likelihood of a system reaching or exceeding a certain damage configuration due to an external stressor, such as a natural disaster. Restoration analysis, on the other hand, examines the speed and efficiency with which a system recovers from a disruptive event. By amalgamating these analyses into one comprehensive framework, we are better equipped to evaluate and quantify the overall resilience of transportation infrastructure.

To compile a robust resilience analysis, the structural responses from numerous infrastructure components are used to determine the DCs of the infrastructure, which are essentially the relationship between demand (how much use the infrastructure gets) and capacity (how much use the infrastructure can handle). These values are then interpreted and linked to restoration information by contrasting the responses to specific repair-based damage states. This correlation enables us to develop a more nuanced understanding of how quickly and efficiently the

infrastructure can be restored following a disruptive event, an essential component of the overall resilience measurement.

As a practical demonstration of the applicability of this framework, it is applied to a real-world case study: the Chemin des Dalles bridge located in Quebec, Canada. By employing the framework to this specific bridge, we can evaluate its resilience and restoration capacities. This helps us to gain practical insights into the effectiveness of the framework and helps to shed light on the specific vulnerabilities and strengths of this particular piece of infrastructure, contributing to an enhanced understanding of how to better design, maintain, and manage such structures in the future.

5.2 Conclusions

The following conclusions can be drawn from this research:

- The proposed framework enables the creation of recovery curves based on actual restoration tasks. This is done by incorporating uncertainties in the restoration process such as task duration, idle time, and resource availability into the resilience assessment.
- Infrastructural restoration duration is significantly affected by these factors. Using the Chemin des Dalles bridge as a case study, it was observed that the presence of idle time and early restoration tasks did not significantly increase functionality after 30 days following an earthquake of high intensity.
- Early in the restoration phase, the bridge's functionality profile is largely determined by the minor DC's recovery curve, which shows rapid functional increase. At the end of the restoration phase (around day 30 onwards), however, the functionality profile is dictated by major DCs with a gradual increase in functionality.

- The damage to the elastomeric bearings on the bridge and the subsequent replacement contributed significantly to major DCs and the total closure of the bridge during restoration. It may be possible to increase the bridge's resilience by repairing or replacing these bearings prior to an event.
- With DCs, the framework incorporates all potential conditions for damage during a hazard and develops recovery curves reflecting the specific performance of the infrastructure. This is more comprehensive than using qualitative system damage states.
- This framework enables the development of resilient curves for infrastructure and the quantification of resilience, as demonstrated by the performance of the bridge when hit by an earthquake that exceeds the NBCC design earthquake.
- In this framework, the resilience surface provides a visual representation of the combined result of fragility and restoration analysis, applicable across various infrastructures.

5.3 Future work

Based on the conclusions derived from the study, the following are recommended areas for future research:

- The current study incorporated uncertainties related to the restoration process such as task duration, idle time, and resource availability. For future studies, it will be beneficial to expand uncertainties in resilience assessments. This could involve exploring uncertainties relating to construction-induced functionality, and further exploration into demand and capacity uncertainty over time.
- The study did not examine how extreme weather conditions affect the efficiency of repair and restoration crews. This could be explored in future research, looking at how weather conditions might affect restoration timelines and the overall resilience of the infrastructure.

- The study found that elastomeric bearings could increase the bridge's resilience following an event if they were repaired or replaced prior to that event. In the future, research could focus on identifying other preemptive mitigation strategies for different infrastructure components and systems. This could include developing predictive maintenance strategies or improving infrastructure design to better withstand specific hazards.

Appendix

Table 7 List of all observed DCs

	LC1	LC2	LC3	RC1	RC2	RC3	LB	LPB	RPB	RB	LAb	RAb
Minor DC1	DS1	DS1	-	-	-	-	-	-	-	-	-	-
Minor DC2	DS1	DS1	DS1	-	-	-	-	DS1	-	-	-	-
Minor DC3	-	-	-	DS1	DS1	DS1	-	-	DS1	DS1	-	-
Minor DC4	DS1	DS1	DS1	DS1	DS1	DS1	DS1	DS1	-	-	-	-
Minor DC5	DS1	DS1	DS1	DS1	DS1	DS1	-	DS1	DS1	DS1	DS1	-
Minor DC6	DS1	DS1	DS1	-	-	-	DS1	-	DS1	-	DS1	DS1
Minor DC7	DS2	DS2	DS2	DS1	DS1	DS1	-	DS1	DS1	-	DS1	DS1
Major DC1	DS1	DS1	DS1	DS1	DS1	DS1	-	-	DS2	-	-	DS2
Major DC2	DS2	DS2	DS2	DS2	DS2	DS2	DS1	DS2	DS1	DS1	DS1	DS2
Major DC3	DS2	DS2	DS2	DS2	DS2	DS2	DS2	DS1	DS2	DS2	DS2	DS1

Notations and abbreviations

DC: damage configuration

DS: damage state

GMTH: ground motion time history

IM: intensity measure

L: lower band of the uniform distribution

LAb and RAb: left and right abutments

LB and RB: left and right bearings

LC and RC: left and right columns

LPB and RPB: left and right pier bearings

N_{DC}: number of damage configurations

N_{DS}: number of damage states

$P[DC_i|IM]$: the probability of the infrastructure being in damage configuration i at the intensity level IM ($i = 1, 2, \ldots, N_{DC}$)

PGA: peak ground acceleration

$P[DS_i|IM]$: the probability of the infrastructure being in damage state i at the intensity level im ($i = 1, 2, \ldots, N_{DS}$)

Q_{safety}: functionality due to structural safety requirement

Q_{sample}: sample recovery curve

Q_{task}: construction-induced functionality

$Q(t)$: functionality profile of the infrastructure over time

$Q[t|DS_i]$: recovery curve of the infrastructure for each specific damage state i over time ($i = 1, 2, \ldots, N_{DS}$)

$Q[t|DC_i]$: recovery curve of the infrastructure for each specific damage configuration i over time

($i = 1, 2, \ldots, N_{DC}$)

R: resilience index

S_C: median

t: time

t_0: the time when hazard hits the structure

t_r: start of the restoration process

t_1: end of the restoration process

U: upper band of the uniform distribution

β_C: dispersion

λ: lognormal distribution parameter (mean of the associated normal distribution)

μ: mean of the normal distribution

μ_d: displacement ductility of the columns

ξ: lognormal distribution parameter (standard deviation of the associated normal distribution)

σ: standard deviation of the normal distribution

References

Abdelmaksoud, A. M., Patel, M. K., Becker, T. C., & Balomenos, G. P. (2022). Parameterized models for prediction of lifetime bearing demands. *Engineering Structures*, *252*, 113649.

Argyroudis, S. A. (2022). Resilience metrics for transport networks: a review and practical examples for bridges. *Proceedings of the Institution of Civil Engineers-Bridge Engineering*, 1–14.

Argyroudis, S. A., & Mitoulis, S. A. (2021). Vulnerability of bridges to individual and multiple hazards-floods and earthquakes. *Reliability Engineering \& System Safety*, *210*, 107564.

Argyroudis, S. A., Nasiopoulos, G., Mantadakis, N., & Mitoulis, S. A. (2020). Cost-based resilience assessment of bridges subjected to earthquakes. *International Journal of Disaster Resilience in the Built Environment*.

Argyroudis S, Mitoulis S, Nasiopoulos G, Mantadakis N, & Mantadakis D. (2019). Resilience of bridges subjected to earthquakes: A case study on a portfolio of road bridges. *2nd International Conference on Natural Hazards & Infrastructure (ICONHIC2019)*.

Aria, M., & Akbari, R. (2013). Inspection, condition evaluation and replacement of elastomeric bearings in road bridges. *Https://Doi.Org/10.1080/15732479.2011.638171*, *9*(9), 918–934. https://doi.org/10.1080/15732479.2011.638171

Artigues, C., Demassey, S., & Neron, E. (2013). *Resource-constrained project scheduling: models, algorithms, extensions and applications*. John Wiley \& Sons.

Atkinson, G. M. (2009). Earthquake time histories compatible with the 2005 National building code of Canada uniform hazard spectrum. *Canadian Journal of Civil Engineering*, *36*(6), 991–1000.

Ayyub, B. M. (2014). Systems resilience for multihazard environments: Definition, metrics, and valuation for decision making. *Risk Analysis*, *34*(2), 340–355.

Balomenos, G. P., Hu, Y., Padgett, J. E., & Shelton, K. (2019). Impact of coastal hazards on residents' spatial accessibility to health services. *Journal of Infrastructure Systems*, *25*(4), 4019028.

Balomenos, G. P., & Padgett, J. E. (2018). Effects of wave loading conditions on the fragility of pile-supported wharves/piers. *Coastal Engineering Proceedings*, *36*, 29.

Banerjee Basu, S., & Shinozuka, M. (2011). Effect of ground motion directionality on fragility characteristics of a highway bridge. *Advances in Civil Engineering*, *2011*.

Bernier, C., Gidaris, I., Balomenos, G. P., & Padgett, J. E. (2019). Assessing the accessibility of petrochemical facilities during storm surge events. *Reliability Engineering \& System Safety*, *188*, 155–167.

Bešinović, N. (2020). Resilience in railway transport systems: a literature review and research agenda. *Transport Reviews*, *40*(4), 457–478. https://doi.org/10.1080/01441647.2020.1728419

Biazar, S., Kameshwar, S., & Balomenos, G. P. (2022). Modal and pushover analysis of concrete bridges with shallow footing subjected to seismic and scour loading. In *Bridge Safety, Maintenance, Management, Life-Cycle, Resilience and Sustainability* (pp. 2138–2145). CRC Press.

Bocchini, P., Decò, A., & Frangopol, D. M. (2012). Probabilistic functionality recovery model for resilience analysis. *Bridge Maintenance, Safety, Management, Resilience and Sustainability*, 1920–1927.

Bocchini, P., Frangopol, D. M., Ummenhofer, T., & Zinke, T. (2014). Resilience and sustainability of civil infrastructure: Toward a unified approach. *Journal of Infrastructure Systems*, *20*(2), 4014004.

Bruneau, M., Chang, S. E., Eguchi, R. T., Lee, G. C., O'Rourke, T. D., Reinhorn, A. M., Shinozuka, M., Tierney, K., Wallace, W. A., & Von Winterfeldt, D. (2003). A framework to quantitatively assess and enhance the seismic resilience of communities. *Earthquake Spectra*, *19*(4), 733–752.

Capacci, L., & Biondini, F. (2020). Probabilistic life-cycle seismic resilience assessment of aging bridge networks considering infrastructure upgrading. *Structure and Infrastructure Engineering*, *16*(4), 659–675.

Chan, R., & Schofer, J. L. (2016). Measuring transportation system resilience: Response of rail transit to weather disruptions. *Natural Hazards Review*, *17*(1), 5015004.

Chandrasekaran, S., & Banerjee, S. (2016). Retrofit optimization for resilience enhancement of bridges under multihazard scenario. *Journal of Structural Engineering*, *142*(8), C4015012.

Cimellaro, G. P., Fumo, C., Reinhorn, A. M., & Bruneau, M. (2009). *Quantification of disaster resilience of health care facilities*. MCEER Buffalo, NY, USA.

Comartin, C. D. (1995). The Hyogoken Nambu Earthquake, Great Hanshin Earthquake disaster, January 17, 1995. *Preliminary Reconnaissance Report*.

Crouse, C. B. (1985). Dynamic response of bridge-abutment-backfill systems. *Proc. Joint US-New Zealand Workshop on Seismic Resistance of Highway Bridges*.

Crow, R., McHaney, S., Holmlund, R., Hall, J., Vivyan, B., Halonen, L., White, L., Lowe, J., Laird, A., Inc., G., Associates, E. S., & Associates, T. (2014). *District 1 Climate Change*

Vulnerability Assessment and Pilot Studies: FHWA Climate Resilience Pilot Final Report. https://doi.org/10.21949/1503647

Cusson, D., & Paultre, P. (1995). Stress-strain model for confined high-strength concrete. *Journal of Structural Engineering*, *121*(3), 468–477.

Decò, A., Bocchini, P., & Frangopol, D. M. (2013). A probabilistic approach for the prediction of seismic resilience of bridges. *Earthquake Engineering \& Structural Dynamics*, *42*(10), 1469–1487.

Echevarria, A., Zaghi, A. E., Christenson, R., & Accorsi, M. (2016). CFFT bridge columns for multihazard resilience. *Journal of Structural Engineering*, *142*(8), C4015002.

FEMA, H. (1999). 99: Technical Manual. *Federal Emergency Management Agency, Washington DC*.

Filosa, G., Plovnick, A., Stahl, L., Miller, R., Pickrell, D. H., & (U.S.), J. A. V. N. T. S. C. (2017). *Vulnerability Assessment and Adaptation Framework, Third Edition*. https://doi.org/10.21949/1503647

Ganin, A. A., Kitsak, M., Marchese, D., Keisler, J. M., Seager, T., & Linkov, I. (2017). Resilience and efficiency in transportation networks. *Science Advances*, *3*(12), e1701079.

Godazgar, B., Balomenos, G., & Tighe, S. (2021). Restoration Curves for Infrastructure: Preliminary Case Study on a Bridge in Quebec. *Proceedings of the Institution of Civil Engineers-Bridge Engineering*, 1–17.

Hall, J. F., Holmes, W. T., & Somers, P. (1994). Northridge earthquake, January 17, 1994. *Preliminary Reconnaissance Report*.

Hambly, E. C. (1991). *Bridge deck behaviour*. CRC Press.

Hollnagel, E., Woods, D. D., & Leveson, N. (2006). *Resilience engineering: Concepts and precepts*. Ashgate Publishing, Ltd.

Huang, Z., Zhang, D., Pitilakis, K., Tsinidis, G., Huang, H., Zhang, D., & Argyroudis, S. (2022). Resilience assessment of tunnels: Framework and application for tunnels in alluvial deposits exposed to seismic hazard. *Soil Dynamics and Earthquake Engineering*, *162*, 107456. https://doi.org/10.1016/J.SOILDYN.2022.107456

Karamlou, A. (2017). *Multi-Scale Methodologies for Probabilistic Resilience Assessment and Enhancement of Bridges and Transportation Systems*. http://preserve.lehigh.edu/etdhttp://preserve.lehigh.edu/etd/2655

Karamlou, A., & Bocchini, P. (2015). Computation of bridge seismic fragility by large-scale simulation for probabilistic resilience analysis. *Earthquake Engineering \& Structural Dynamics*, *44*(12), 1959–1978.

Karamlou, A., & Bocchini, P. (2017a). From component damage to system-level probabilistic restoration functions for a damaged bridge. *Journal of Infrastructure Systems*, *23*(3), 4016042.

Karamlou, A., & Bocchini, P. (2017b). Functionality-fragility surfaces. *Earthquake Engineering and Structural Dynamics*, *46*(10), 1687–1709. https://doi.org/10.1002/eqe.2878

Mackie, K. R., Kucukvar, M., Tatari, O., & Elgamal, A. (2016). Sustainability metrics for performance-based seismic bridge response. *Journal of Structural Engineering*, *142*(8), C4015001.

Mackie, K. R., Wong, J.-M., & Stojadinovic, B. (2008). Integrated Probabilistic Performance-Based Evaluation of Benchmark Reinforced Concrete Bridges. In *Pacific Earthquake Engineering Research Center* (Issue January).

Mazzoni, S., McKenna, F., Scott, M. H., Fenves, G. L., & others. (2006). OpenSees command language manual. *Pacific Earthquake Engineering Research (PEER) Center*, *264*, 137–158.

McKay, M. D., Beckman, R. J., & Conover, W. J. (2000). A comparison of three methods for selecting values of input variables in the analysis of output from a computer code. *Technometrics*, *42*(1), 55–61.

Minaie, E., & Moon, F. (2017). Practical and simplified approach for quantifying bridge resilience. *Journal of Infrastructure Systems*, *23*(4), 4017016.

Mitoulis, S. A., Argyroudis, S. A., Loli, M., & Imam, B. (2021). Restoration models for quantifying flood resilience of bridges. *Engineering Structures*, *238*(February), (accepted). https://doi.org/10.1016/j.engstruct.2021.112180

National Research Council of Canada (NRCC). (2015). *National Building Code of Canada, 2015*. National Research Council Canada, Ottawa, ON, Canada.

Noade, B. M., & Becker, T. C. (2019). Probabilistic framework for lifetime bridge-bearing demands. *Journal of Bridge Engineering*, *24*(7), 4019065.

Omer, M., Mostashari, A., Nilchiani, R., & Mansouri, M. (2012). A framework for assessing resiliency of maritime transportation systems. *Maritime Policy \& Management*, *39*(7), 685–703.

Padgett, J. E., & DesRoches, R. (2007). Bridge functionality relationships for improved seismic risk assessment of transportation networks. *Earthquake Spectra*, *23*(1), 115–130.

Padgett, J. E., Nielson, B. G., & DesRoches, R. (2008). Selection of optimal intensity measures in probabilistic seismic demand models of highway bridge portfolios. *Earthquake Engineering \& Structural Dynamics*, *37*(5), 711–725.

Porter, K. A. (2004). *A survey of bridge practitioners to relate damage to closure.*

Rinaldi, S. M., Peerenboom, J. P., & Kelly, T. K. (2001). Identifying, understanding, and analyzing critical infrastructure interdependencies. *IEEE Control Systems Magazine*, *21*(6), 11–25.

Rojahn, C., & Sharpe, R. L. (1985). *Earthquake damage evaluation data for California*. Applied technology council.

Roy, N., Paultre, P., & Proulx, J. (2010). Performance-based seismic retrofit of a bridge bent: Design and experimental validation. *Canadian Journal of Civil Engineering*, *37*(3), 367–379.

Sharma, N., Tabandeh, A., & Gardoni, P. (2018). Resilience analysis: A mathematical formulation to model resilience of engineering systems. *Sustainable and Resilient Infrastructure*, *3*(2), 49–67.

Siqueira, G. H., Tavares, D. H., & Paultre, P. (2014). Seismic fragility of a highway bridge in Quebec retrofitted with natural rubber isolators. *Revista IBRACON de Estruturas e Materiais*, *7*(4), 534–547.

Tavares, D. H., Suescun, J. R., Paultre, P., & Padgett, J. E. (2013). Seismic Fragility of a Highway Bridge in Quebec. *Journal of Bridge Engineering*, *18*(11), 1131–1139. https://doi.org/10.1061/(asce)be.1943-5592.0000471

Torbol, M., & Shinozuka, M. (2014). The directionality effect in the seismic risk assessment of highway networks. *Structure and Infrastructure Engineering*, *10*(2), 175–188.

Wilkinson, S., Free, M., Grant, D., Boon, D., Paganoni, S., Mason, A., Williams, E., Fraser, S., & Haskell, J. (2011). The Christchurch, New Zealand earthquake of 22 February 2011. *Report No., Earthquake Field Investigation Team, Institution of Structural Engineers*.

Wilson, J. C. (1988). Stiffness of non-skew monolithic bridge abutments for seismic analysis. *Earthquake Engineering \& Structural Dynamics*, *16*(6), 867–883.

Yilmaz, M. F., Ozakgul, K., & Caglayan, B. O. (2021). Seismic fragility analysis of multi-span steel truss railway bridges in Turkey. *Structure and Infrastructure Engineering*, 1–18.

Zobel, C. W. (2011). Representing perceived tradeoffs in defining disaster resilience. *Decision Support Systems*, *50*(2), 394–403.